A Generalized Water Retention Model for Geosynthetic Clay Liners

Zhi Chong Lau[1]; Abdelmalek Bouazza[2]; Ning Lu, F.ASCE[3]; and Will P. Gates[4]

Abstract: The composite nature of geosynthetic clay liners and the contrasting water retention behavior of its bentonite and geotextile components has presented a unique challenge that current water retention models do not fully address. This paper proposes a new water retention model that can accurately describe the bimodal behavior of geosynthetic clay liners across the entire suction range (10^{-2}–10^{6} kPa) on the adsorption path. The model was formulated based on the pore structures and dominant suction regimes present in geosynthetic clay liners. In addition to the soil adsorptive and capillary water, it incorporates the geotextile capillary regime, which encompasses the pore water fraction in the geotextile, bentonite extrusion into the geotextile, and additionally, any volume changes due to bentonite swelling (including polymer effects). The parameters defined in this conceptual model describe the physical characteristics of bentonite and the geotextile fraction in the geosynthetic clay liner (GCL). The proposed model's performance was assessed and validated using extensive experimental water retention data sets. The statistical analysis indicated that the proposed model provides a better fit than other models, especially in the low-suction range, and is adept at predicting the water retention behavior of the geosynthetic clay liners on the wetting path. **DOI: 10.1061/(ASCE)GT.1943-5606.0002933.** *© 2022 American Society of Civil Engineers.*

Author keywords: Geosynthetics; Geosynthetic clay liners (GCLs); Fitting models; Water retention curves; Adsorption; Capillarity.

Introduction

Geosynthetic clay liners (GCLs), composed of bentonite enclosed between two geotextile sheets through needle punching, are typically used together with geomembranes to form composite liners to prevent or slow the migration of contaminants from waste containment facilities (Shackelford et al. 2000; Bouazza 2002; Hornsey et al. 2010; Bouazza and Bowders 2010; Bouazza and Gates 2014; Rowe 2014; Bouazza et al. 2014; Scalia et al. 2014; Mazzieri and Di Emidio 2015; Touze-Foltz et al. 2016; Bouazza et al. 2017b; Gates et al. 2020; Tian et al. 2019; Ghavam-Nasiri et al. 2020; Bouazza 2021; Rowe and AbdelRazek 2021).

Understanding the hydraulic properties of GCLs is critical because they are one of the significant factors affecting a GCL's engineering performance. These hydraulic properties include the water retention curve (WRC) and hydraulic conductivity. Both can be directly linked to the amount of moisture uptake by the bentonite component of the GCL from the subsoil material, i.e., the hydration level required to ensure the bentonite forms a sealing barrier. Previous studies have indicated that GCLs should achieve a prehydration gravimetric water content (GWC) > 100% before exposure to solutes (Daniel 1993; Vasko et al. 2001; Bouazza and Gates 2014; Liu et al. 2015) or more than 70% GWC for gas migration applications (Rouf et al. 2016b; Bouazza et al. 2017c) to ensure the bentonite is adequately swollen for optimum hydraulic performance. However, achieving these hydration levels in the field is not straightforward because GCL hydration from a given subsoil is dependent on several factors, including GCL type, subsoil type and mineralogy, pore water chemistry, and operating conditions (Rayhani et al. 2011; Rowe et al. 2011; Anderson et al. 2012; Chevrier et al. 2012; Bradshaw et al. 2013; Sarabian and Rayhani 2013; Barclay and Rayhani 2013; Bouazza et al. 2017a; Acikel et al. 2018b; Carnero-Guzman et al. 2021; Lau et al. 2022b).

The effect of the aforementioned factors can be explained within the framework of the fundamental constitutive relationship between suction and water content of the GCL. This relationship, also known as the water retention curve, is an invaluable tool that can be used to understand water movement and distribution within the GCL and its surroundings. However, due to the composite nature of the GCL and vastly contrasting water retention behavior of its components (i.e., bentonite and geotextiles), it has proven to be a challenging task to quantify the WRC across its entire suction range (Abuel-Naga and Bouazza 2010; Beddoe et al. 2011; Acikel et al. 2018a, 2022; Tincopa et al. 2020; Tincopa and Bouazza 2021). The measurement of the WRC has become even more complicated with the emergence of polymer-enhanced GCLs. These polymer enhancements further affect the water retention behavior of GCLs depending on the polymer type and dosage, particularly in the low-suction range (Lau et al. 2022a).

In practice, experimental data are fitted using water retention models to produce a smooth and continuous water retention curve that describes the material hydraulic behavior over an extensive range of suctions. Nonetheless, the WRC of GCLs presents unique challenges that current models do not fully address. The empirical models most commonly used for GCLs are the van Genuchten (vG)

[1]Ph.D. Student, Dept. of Civil Engineering, Monash Univ., 23 College Walk, Melbourne, VIC 3800, Australia. Email: lauzhichong@gmail.com

[2]Professor, Dept. of Civil Engineering, Monash Univ., 23 College Walk, Melbourne, VIC 3800, Australia (corresponding author). ORCID: https://orcid.org/0000-0003-1768-1503. Email: malek.bouazza@monash.edu

[3]Professor, Dept. of Civil and Environmental Engineering, Colorado School of Mines, Golden, CO 80401. ORCID: https://orcid.org/0000-0003-1753-129X. Email: ninglu@mines.edu

[4]Associate Professor, Institute for Frontier Materials, Deakin Univ., Melbourne, VIC 3125, Australia. ORCID: https://orcid.org/0000-0001-7388-0289. Email: will.gates@deakin.edu.au

Note. This manuscript was submitted on October 26, 2021; approved on August 19, 2022; published online on October 12, 2022. Discussion period open until March 12, 2023; separate discussions must be submitted for individual papers. This paper is part of the ***Journal of Geotechnical and Geoenvironmental Engineering***, © ASCE, ISSN 1090-0241.

model (Van Genuchten 1980) and the Fredlund and Xing (FX) model (Fredlund and Xing 1994). The modeling needs to represent different water retention mechanisms over a wide suction range, including adsorption water in bentonite at the high-suction range, capillary water in bentonite at the intermediate-suction range, and capillary water in the geotextile at the low-suction range. The advent of polymer-modified bentonites has made the establishment of highly predictable water retention models for GCLs even more complex.

This paper presents a new water retention model that can accurately describe the bimodal behavior of GCLs, including polymer-enhanced GCLs, across the full suction range. The model is formulated based on the pore water fractions and dominant suction regimes in the GCL. The conceptual framework of the water retention mechanisms in GCLs is presented to provide context for the various parameters used in the model. The proposed model was validated against experimental data from different GCLs and compared with existing models to evaluate its adequacy in describing GCL water retention behaviors.

Materials

Five different needle-punched GCLs were investigated in the current study; they are referred to herein as GCL1, GCL2, GCL3, GCL4, and GCL5, respectively. GCL1 contained polymer-enhanced sodium powder bentonite. GCL2 had an unmodified granular sodium bentonite core. All other GCLs (GCL3–GCL5) contained granular sodium bentonites enhanced with different polymer modifications. The characteristics and properties of these five GCLs and their bentonites were reported in detail by Lau et al. (2022a) and are summarized in Table 1.

The representative mass per unit area measured as per ASTM D5993 (ASTM 2018a) and the as-received water content of the GCLs were established using a sample size of 24 specimens randomly taken from each GCL roll. The representative mass per unit area of each GCL was based on the most frequent range (mode) identified in the mass per unit area histogram data set relevant to each GCL type. The as-received water content is reported as the average of all water content values for each GCL type. The peel strength of the GCLs was measured following ASTM D6496 (ASTM 2020). The maximum GWC of the GCLs (w_{sat}) were attained by placing the specimens on a saturated porous stone under 2 kPa vertical stress and recording GWC changes until final equilibrium GWCs were achieved. The GWCs recorded at equilibrium were considered the maximum GWC attained by the GCLs and used as the benchmark for GCLs under quasi-saturation conditions ($S = 100\%$) (Acikel et al. 2018b). Thus, these measurements were considered representative of the saturated GCLs GWCs where suction is deemed equal to zero.

The polymer contents of the enhanced bentonite in GCL3–GCL5 were estimated using loss on ignition (LOI) tests (Scalia et al. 2014; Tian et al. 2016, 2019; Chen et al. 2019; Wireko et al. 2020). However, for GCL1, the GCL manufacturer provided the pure polymer fraction and the nonmodified base bentonite. The base bentonite and polymer's relative mass loss were considered to estimate GCL1 polymer content. The LOI of the nonmodified bentonite in GCL2 (0.8%) formed the baseline for GCL3, GCL4, and GCL5. It was attributed to the removal of strongly bound water (Grim 1968), carbonates, and other organic materials possibly associated with the bentonite (Scalia et al. 2014; Tian et al. 2016, 2019). Because the base polymers for GCL3, GCL4, and GCL5 were not available (proprietary information), complete combustion of the polymer additives was assumed to have occurred at 550°C (Tian et al. 2016, 2019; Chen et al. 2019; Wireko et al. 2020). Consequently, it is postulated that the actual polymer content may be underestimated using this polymer quantification method.

The term bentonite presented in this paper always refers to the bentonite core as present in a given GCL; polymer, if present, was not separated from the bentonite. Index properties such as swell index and fluid loss were conducted on the bentonite component extracted from the GCLs following the procedures outlined in

Table 1. Characteristics and properties of geosynthetic clay liners

Properties	GCL1	GCL2	GCL3	GCL4	GCL5
Bonding	Needle punched, thermally treated	Needle punched	Needle punched	Needle punched	Needle punched
Bentonite type	Polymer-enhanced sodium powder	Sodium granular	Polymer-enhanced sodium granular	Polymer-enhanced sodium granular	Polymer-enhanced sodium granular
Polymer type	Linear	—	Linear	Cross-linked	Cross-linked
Estimated polymer content (%)	1.6[a]	—	3.0	9.9	4.4
Carrier geotextile type	Nonwoven + woven scrim reinforced	Nonwoven	Nonwoven + woven composite	Nonwoven	Nonwoven
Carrier geotextile mass per unit area (kg/m^2)	0.570	0.200	0.308	0.200	0.200
Cover geotextile type	Nonwoven	Nonwoven	Nonwoven	Nonwoven	Nonwoven
Cover geotextile mass per unit area (kg/m^2)	0.350	0.200	0.300	0.300	0.200
Representative GCL mass per unit area (kg/m^2)	5.9–6.1	6.4–6.6	5.3–5.6	5.1–5.4	5.2–5.4
Average peel strength (N/m)	1,350	1,388	3,137	4,523	2,860
Average as received gravimetric water content (%)	7.3	9.2	6.3	7.4	7.9
Maximum GWC, w_{sat} (%)	188	151	183	223	214
Swell index (mL/2g)	33.1	25.6	36.4	55.8	45.5
Fluid loss (mL)	13.8	12.4	5.9	8.7	9.3
Solution retention capacity (mL/g)	6.4	6.8	8.1	8.7	10.0
Cation exchange capacity[b] (cmol/kg)	85	76	78	79	84

[a]Estimation takes into consideration the relative mass loss of its base polymer.
[b]Performed by Mineralogical Services, CSIRO Minerals, Adelaide, South Australia, Australia.

Table 2. Mineralogical composition of the bentonite in GCLs

Mineralogical composition	GCL1	GCL2	GCL3	GCL4	GCL5
Quartz (%)	12	1	1	1	1
Cristobalite/opal CT (%)	8	12	12	12	12
Montmorillonite (%)	74	81	80	80	82
Albite/anorthite (%)	4	4	4	4	3
Kaolin (%)	1	—	—	—	—
Mica (%)	—	1	1	1	1
Calcite (%)	<1	<1	1	1	<1
Zeolite (%)	1	1	1	1	1

Note: Performed by Mineralogical Services, CSIRO Minerals, Adelaide, South Australia, Australia. Opal CT = opaline cristobalite–tridymite.

ASTM D5890 (ASTM 2018b) and ASTM D5891 (ASTM 2016), respectively. The solution retention capacity of the bentonite component was measured following the methods outlined by Lee and Shackelford (2005) and Fehervari et al. (2019). The measurements of cation exchange capacity (CEC) were made using the barium chloride ($BaCl_2$) compulsive exchange method (Sumner and Miller 1996) with barium (Ba) analysis by X-ray fluorescence (Norrish and Hutton 1969; Battaglia et al. 2006). The mineralogical composition was determined using quantitative X-ray diffraction (XRD) analysis and is presented in Table 2.

Experimental Methods and Data

The wetting path of the GCL water retention curve presents the hydraulic behavior of the GCL from a very dry state at a suction value of >500 MPa up to its assumed fully saturated state of 0.1 kPa. Different measurement techniques were employed to capture the GCL water retention curve across a wide suction range. The measurement methods used in this study included the vapor sorption analyzer (VSA) (5–500 MPa), the dewpoint potentiometer (1–140 MPa), and the filter paper method (0.1–146 kPa), specifically the initial wet contact filter paper tests (IWCFPT). These methods target a specific suction range; combined, they provide the entire water retention curve on the wetting path. The GCLs' water retention experimental procedures and measurement data were presented and discussed in detail by Lau et al. (2022a); only a summary is given in the following section.

Using the three aforementioned methods, an extensive water retention curve of the various GCLs was constructed, as shown in Figs. 1(a and b). It can be observed that GCLs generally exhibit a bimodal behavior rather than a unimodal sigmoid curve. At the intermediate- to high-suction range (>1,000 kPa), the water retention curve mostly follows a similar path across the various GCL types. This curve coalesces above 5,000 kPa for all GCLs, indicating that bentonite mineralogy controls the high-suction regime. The curve diverges for the different GCLs between about 700 to 5,000 kPa due to differences in the pore and microstructure of the bentonite core and the influence of polymers, as has been discussed recently by Lau et al. (2022a). The variation in water retention is more apparent in the low-suction region (<700 kPa), where its behavior depends on the GCL structure and the bentonite type (i.e., presence of polymer, polymer type, and loading). These factors impact water uptake by the GCL and strongly influence the maximum GWC achieved, as shown in Fig. 1(a). Volume change due to bentonite swelling along the wetting path is factored in by expressing the water retention curve volumetrically, as shown in Fig. 1(b).

The differences in the volume-dependent WRC across the various GCLs are more subtle. The WRC data shown in Fig. 1(b) illustrate a bimodal shape with at least four different slopes: between the suction ranges of 0.1–0.3, 0.3–1,000, 1,000–4,000, and >4,000 kPa. This indicates the GCLs' WRC is a function of multiple distinct pore series corresponding to a bimodal water retention behavior (Burger and Shackelford 2001; Zhang and Chen 2005; Satyanaga et al. 2013). Thus, to fully capture the water retention behavior of composite materials like a GCL, it has to be explained through the perspective of the pore structures present and the governing suction mechanisms. Fig. 2 illustrates the mechanisms governing the water retention of a GCL using data from GCL1 as an example.

Water Fractions within Geosynthetic Clay Liners

The bimodal WRC observed in Fig. 1 can be attributed to the composite nature of GCLs, where the differences in the pore sizes of its constituents are in the orders of magnitude. The apparent opening size of geotextiles is generally within 0.1–0.2 mm (Bouazza et al. 2006a, b). On the other hand, depending on the granularity of the bentonite fraction, the inter-grain pore size can range from 0.1 to 30 μm (Seiphoori et al. 2016; Liu et al. 2020). Additionally, many researchers have characterized bentonite itself as having a dual pore structure (Gens and Alonso 1992; Alonso et al. 1999; Sanchez et al. 2006, 2016; Delage 2007; Villar and Lloret 2008; Romero et al. 2011; Seiphoori et al. 2014; Navarro et al. 2015; Cui 2017; Acikel et al. 2018b, a). Thus, when viewed in its entirety, the GCL is best described with a trimodal pore structure that includes the geotextile pores, the bentonite interaggregate pores deemed to be the bentonite macropores, and the bentonite intra-aggregate pores referred to as the bentonite micropores (Acikel et al. 2018b, 2020; Gates et al. 2021).

The fundamental understanding of pore structures offers a framework for describing the suction regime dictating water retention in GCL. It also facilitates the conceptualization of a fully saturated GCL where the total water content is represented by its total porosity. Porosity can be quantified by the various pore water fractions consisting of the geotextile capillary water, bentonite capillary water, and bentonite adsorption water, as illustrated in Fig. 3. However, although the pore-size distribution of the constituent elements dictates total capillary water behavior, the adsorption water is dependent upon the mineralogical and chemical composition of the bentonite.

Furthermore, capillary water and adsorption water are influenced subtly when polymer modifications are present due to the diverse array of polymer products available with distinct water retention mechanisms. Nonetheless, this framework can adequately characterize the general water retention curve model for GCLs. A more extensive discussion of the water retention behavior and relevant suction mechanism of GCLs has been given by Lau et al. (2022a).

Bentonite Adsorption Water

The bentonite core primarily governs the water retention behavior of GCLs at the high-suction range (Carnero-Guzman et al. 2019; Bouazza and Rouf 2021; Tincopa and Bouazza 2021). In this suction region, the upper-bound suction that marks the onset of bentonite adsorption water is the highest suction of the bentonite. This unique parameter has mainly been considered a function of the bentonite mineralogy and cation type (Jensen et al. 2015; Lu and Khorshidi 2015). The absorbed water suction regime for sodium bentonite concludes at the suction value corresponding to the three- or four-layer hydrated state (Norrish 1954; Laird 1996). The total bentonite adsorption water comprises the tightly adsorbed water

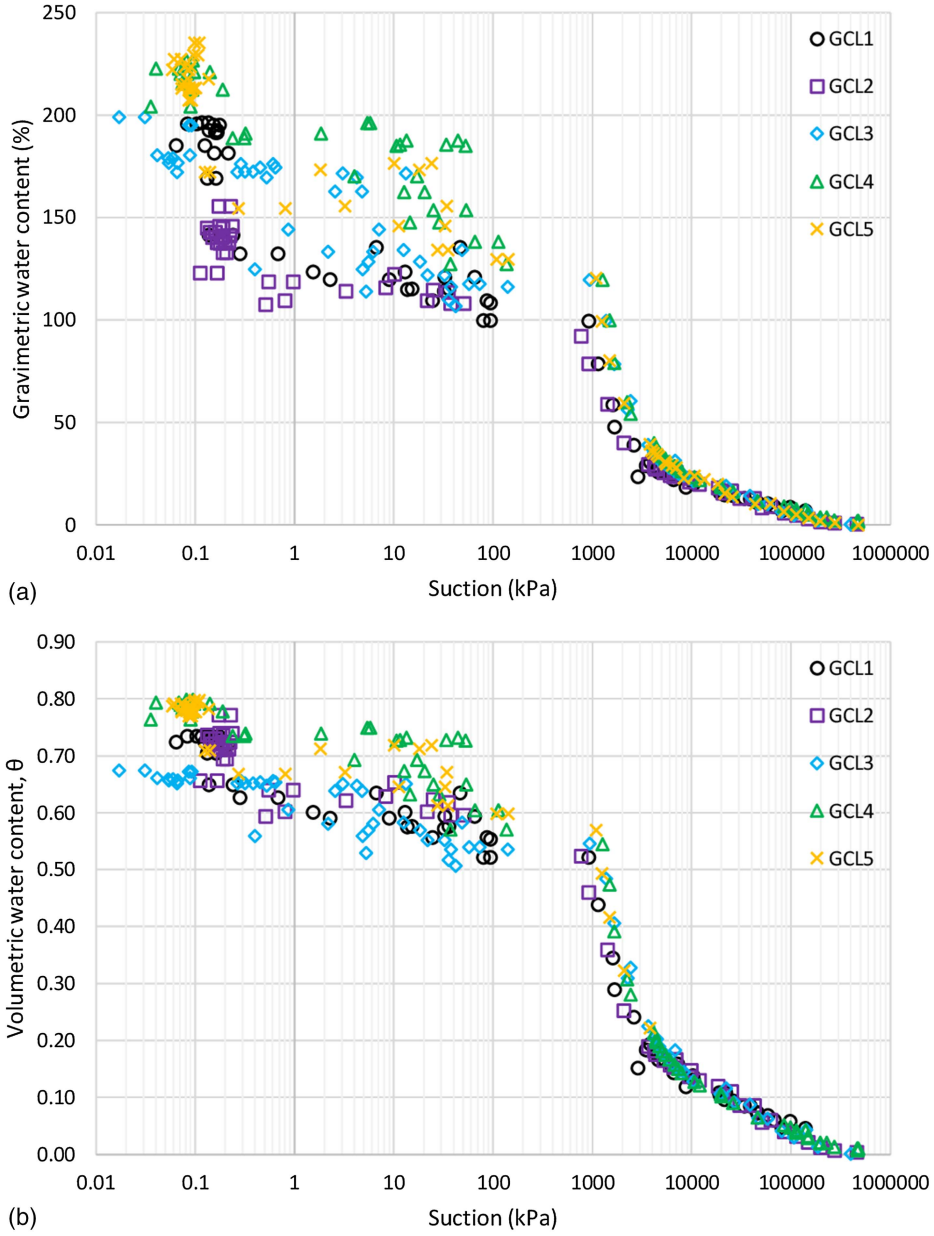

Fig. 1. Experimental data for all the GCL water retention curves shown (a) gravimetrically; and (b) volumetrically.

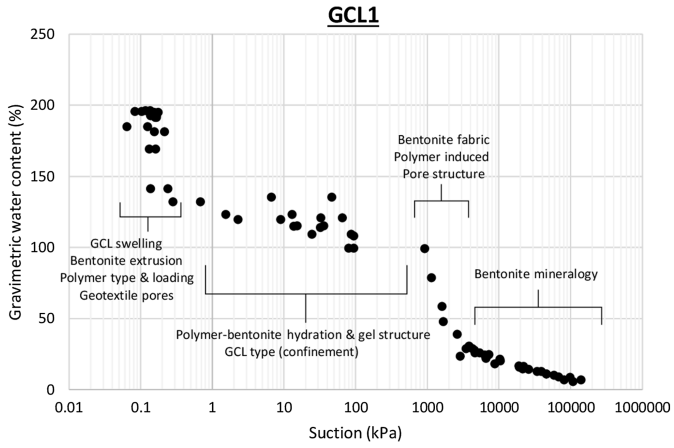

Fig. 2. Governing mechanisms governing the water retention of a GCL. Example used is GCL1.

and the adsorbed film. Thus, the lower suction boundary for the adsorbed film regime, and consequently, the maximum adsorption water in the system, was demarcated by the total adsorption capacity, proposed by Revil and Lu (2013). Like the highest suction parameter, the total bentonite adsorption capacity is unique and depends on mineralogy (Tuller and Or 2005; Lu 2016; Rouf et al. 2016a).

Bentonite Capillary Water

The mesopores and macropores in the bentonite core largely dictate water sorption behavior within the capillary water retention regime of the GCL. The commencement of the bentonite capillary regime is typically demarcated by either the pore water cavitation suction or the residual capillary suction obtained from the water retention curve (Fredlund and Xing 1994; Or and Tuller 2002; Frydman and Baker 2009). The consensus is that the cavitation process occurs progressively over a range of suctions and is best

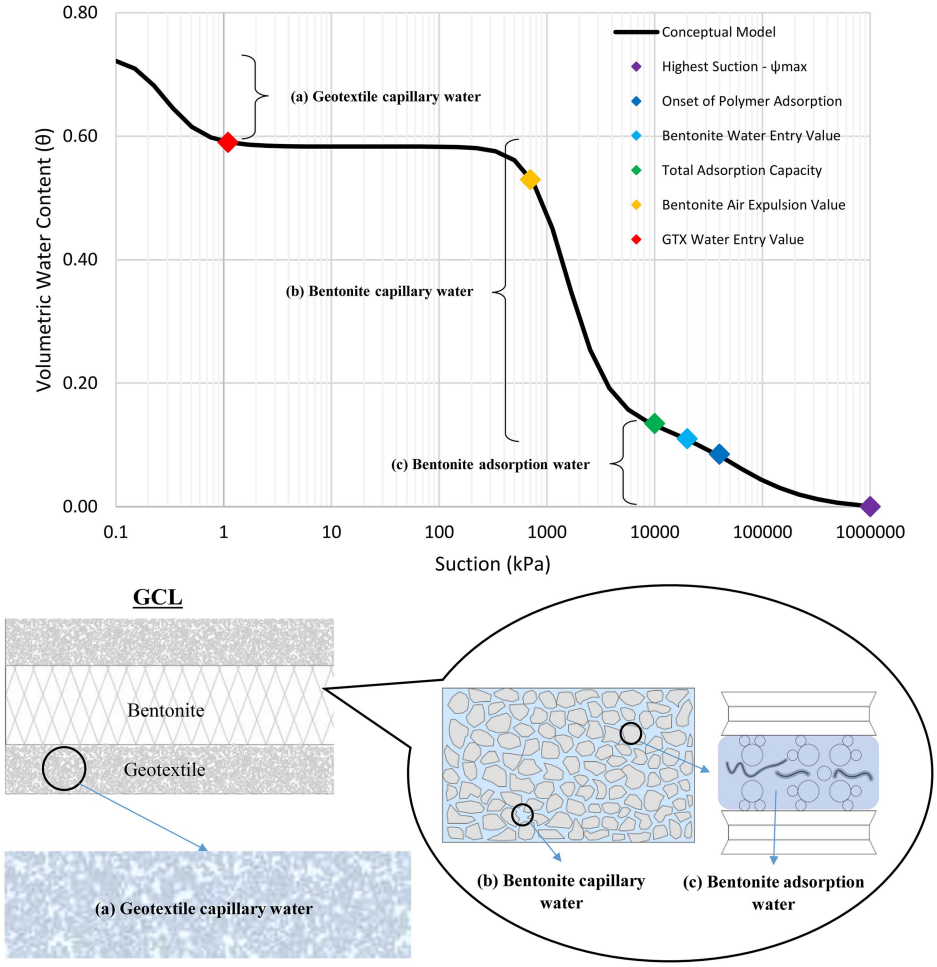

Fig. 3. Conceptualization of the GCL WRC representing the various water fractions making up a fully saturated GCL.

described using a distribution function (Herbert et al. 2006; Lu 2016). Most studies on water cavitation in soil mechanics were investigated under desorption conditions. In contrast, it is assumed for the wetting path that the onset of capillary connection develops at a suction less than its pore water cavitation suction.

Another valid parameter that can be graphically measured from the water retention curve to delineate the capillary regime and adsorption regime is the water entry value (WEV). It is the mean water entry suction value at which capillary connections form between particles in the bentonite macropores and is measured as the suction value at the intersection point between the tangent line of the capillary regime slope and the straight line approximating the high suction adsorption regime (Yang et al. 2004; Acikel et al. 2018b). Finally, as more water migrates into the GCL, the bentonite swells and entrained air is expelled from the pores until it becomes fully saturated. The suction at which this occurs is the air expulsion value (AExV) on the WRC wetting path obtained graphically and is similar to the air entry values (AEV) measured on the drying path. Suctions around the AExV demarcate the region where the bentonite in the GCL transitions to a fully saturated state (Pasha et al. 2017).

Geotextile Capillary Water

The fraction described as geotextile capillary water mobilizes in the low-suction range. Because the geotextile pores are orders of magnitude larger than even the interparticle bentonite pores, the geotextile capillary action can manifest in the form of a separate slope segment of the water retention curve within the low-suction range. It can be observed from the WRC data shown in Fig. 1 that the GCLs experienced an increase in volumetric water content around the suction range of 0.1–0.3 kPa, which is consistent with the values reported in the literature for geotextiles (Iryo and Rowe 2003; Bouazza et al. 2006a, b). Thus, the slope change in the WRC provides a parameter to delineate the onset of geotextile capillary water. However, the transition from bentonite capillary regime to geotextile capillary regime is not strictly a stepwise process but rather a gradual process impacted by factors like the type of geotextiles, type of fiber bonding, presence of polymer, and if so, type of polymer.

Nonetheless, the overall volume proportion of geotextile pores is smaller than the bentonite pores in the GCL. It can be observed from Fig. 1(b) that the capillary water uptake at suctions lower than the air expulsion value of the bentonite is typically within the ranges of 0.1–0.2 volumetric water content (VWC), which is smaller compared with the bentonite fraction (0.5–0.6 VWC). Additionally, when comparing the GCL WRCs in Figs. 1(a and b), the water content increase in the geotextile regime is more apparent when observed in terms of GWC. This difference is due to the large volume change that occurs due to the bentonite swelling. Although the geotextile fibers restrict the bentonites from free swelling, the high swelling pressure at low suctions can cause the fibers to stretch, resulting in the GCL volume change that is accounted for volumetrically. Furthermore, the increase in water

content can also be attributed to the bentonite intrusion into the geotextile pores, as shown by Gates et al. (2018). For GCLs with polymer-modified bentonite, polymer elution (linear polymer) or polymer extrusion (cross-linked polymers) from the geotextiles must be considered.

Polymer Adsorption Water

The water retention behavior of GCLs becomes even more intricate when also considering the role of polymer enhancements, which have garnered some popularity in applications where exposure to aggressive leachates prevails or as a solution to minimize downslope bentonite erosion in GCLs. Nonetheless, within the context of the water retention model presented in the current study, the water fraction attributable to polymer adsorption was evaluated as part of bentonite and geotextile capillary water. It was assumed that any changes to hydration behavior due to the polymer bentonite interactions are reflected in the resulting bentonite water fractions, as shown in Fig. 1(a).

Background on GCL Water Retention Curve Modeling

The range of suctions encompassing the water retention behavior of GCLs spans several orders of magnitude (0.01 to 10^6 kPa), requiring multiple measurement techniques to cover different suction ranges to establish the full WRC. Its complexity, in addition to the time- and cost-intensive nature of these experiments, makes establishing a continuous WRC populated using only measured data highly prohibitive. Thus, in practice, discrete points of measured data obtained are used in conjunction with appropriate soil-water retention curve models for curve-fitting analysis to produce a smooth and continuous WRC that can best simulate the water retention behavior of the GCL based on the experimental data input. Empirical models like the vG model (Van Genuchten 1980) and FX model (Fredlund and Xing 1994) are most commonly used to describe the WRC data for GCLs. These models are fitted to the measured experimental data using a least-squares analysis. All the parameters in these models are obtained through the fitting process except for the saturated volumetric water content (θ_s), which has to be measured experimentally. The fitting parameters, obtained based on the empirical data, can provide insight into specific soil-water characteristics like the air entry, water entry, and air expulsion values, pore-size distribution, and residual suction.

When attributing physical interpretations to the fitting parameters for the FX and vG models, the consensus is that the air entry value and pore-size distribution are well defined by these parameters (a, m, and n), whereas the correlation of θ_r and ψ_r to the residual zone is relatively ill-defined. Furthermore, the fitting parameters intrinsic to both these models were obtained from the best-fit curve based on the shape of the measured GCL WRC data rather than on a theoretical understanding of the water retention mechanism of the GCL. Thus, although these fitting curves can provide a representative model of the GCL water retention behavior, they do not distinguish between the contributory fractions in the total pore water volume, which, as explained in previous sections, is composed of the adsorption water and the capillary water. These drawbacks were addressed by the WRC model proposed by Revil and Lu (2013) (referred to herein as RL) and subsequently by Lu (2016).

The Revil and Lu (2013) model differentiates itself from the FX and vG models. Its fitting equation was based on a theoretical understanding of the various water retention regimes that govern the material's hydraulic behavior. It applies a principle of local matric suction equilibrium where the total pore water volume in the material can be explicitly categorized into adsorptive and capillary water. Therefore, the total pore water volume can be expressed

$$\theta(\psi) = \theta_a(\psi) + \theta_c(\psi) \tag{1}$$

where θ_a = adsorption water; and θ_c = capillary water at a given suction. The capillary water was described by adapting the vG model where the residual water content (θ_r) was replaced by the adsorption water (θ_a) in the system. The adsorptive water was described using the Freundlich model and rearranged using Kelvin's equation. It was written

$$\theta_a(\psi) = \theta_{a\max}\left[\exp\left(-\frac{M_v\psi}{RT}\right)\right]^{\frac{1}{m}} \tag{2}$$

where $\theta_{a\max}$ = total adsorption water capacity; M_v =molar volume of water; R = universal gas constant; and T = absolute temperature (K). The m parameter was redefined to represent the adsorption strength controlled by its mineral composition.

The RL model's limitations are that it cannot define a thermodynamic equivalent suction value of a zero-humidity condition. Thus, it cannot predict a unique maximum suction at which the adsorptive water, and by extension, the total water content, is zero for the material. Furthermore, the RL model underestimates the intrinsically adsorptive water, as described in Kelvin's equation, where the bulk of adsorption is limited to occurring below 137 MPa regardless of the soil type. Although this can be calibrated through other parameters, it can often lead to capillary water overprediction at very high suctions.

The model proposed by Lu (2016) builds on the work presented by Revil and Lu (2013), where it addresses some of the challenges present. The Lu (2016) model changed the denominator in the exponent to a fitting parameter, $\psi_{\max}$, which describes the maximum suction at which water content is zero. This alleviates the underestimation of adsorptive water and ensures that adsorption in this model occurs below its highest suction. The model was also adapted into a closed-form equation to satisfy the physical constraint where the highest suction corresponds with a completely dry condition (water content is zero).

The equation developed by Lu (2016) to describe adsorptive water (θ_a) is expressed

$$\theta_a(\psi) = \theta_{a\max}\left\{1 - \left[\exp\left(1 - \frac{\psi_{\max}}{\psi}\right)\right]^m\right\} \tag{3}$$

where ψ = given suction; $\theta_{a\max}$ = total adsorption water capacity; $\psi_{\max}$ = maximum suction value for the GCL; and m = fitted parameter relating to adsorption strength or the rate of adsorption.

Lu (2016) also considered the intricacies of the cavitation phenomenon in the model for predicting capillary water, which can alleviate the RL model's deficiencies. Although the understanding of cavitation physics is still subject to ongoing research, there is a consensus that there is a considerable variation in a material's cavitation suction, meaning it occurs in a gradual process, and it is most appropriately described using a probability distribution function (Herbert et al. 2006; Lu 2016; Luo and Lu 2021). Thus, Lu (2016) adapted the capillary water equation in the RL model by introducing the cumulative distribution function, which describes the probabilistic nature of water condensation.

The equation for capillary water (θ_c) as proposed by Lu (2016), is an extension of the vG model and is presented as follows:

$$\theta_c(\psi) = \frac{1}{2}[\theta_s - \theta_a(\psi)] \times \frac{\left[1 - \text{erf}\left(\frac{\psi - \psi_c}{\sqrt{2}\sigma_c}\right)\right]}{[1 + (\alpha\psi)^n]^{1-\frac{1}{n}}} \quad (4)$$

where θ_s = measured saturated water content; ψ_c = mean cavitation suction; σ_c = cavitation deviation proposed to be $0.5\psi_c$ (Herbert et al. 2006); α = parameter indicating the inverse of AEV; and n = parameter linked to the pore-size distribution of GCL.

Inadequacies of Current Models for GCLs

The various models presented in the preceding section are all unimodal fitting equations best used to describe porous materials with singular porosity structures. However, GCLs are comprised of multiple components with vastly different pore sizes. Thus, other factors such as their structure and polymer presence (if any) can affect their water retention behavior. The difficulties in attaining accurate low-suction measurements and the comparatively small impact of geotextiles on the overall GCL water retention behavior meant that experimental data for GCLs on the wetting path reported in current literature usually terminated at 10–100 kPa. Although this behavior typically covers the regions where the bentonite component is dominant, it does not fully describe the GCL water retention behavior.

Beddoe et al. (2011) fitted wetting path data of four different GCLs using the FX model to describe primarily the bentonite component of the GCL, which is appropriate given the suction range studied in their work. However, the low-suction range (<10 kPa) was omitted, and their approach assumed that the curve trended unimodally toward the saturated water content after the air expulsion value of the bentonite. Similarly, Acikel et al. (2018a) fitted their experimental data (measured to >100 kPa) on the wetting path using the FX model extended to 10 kPa using an experimentally determined saturated GWC parameter. Although these approaches adequately depicted the bentonite dominant suction region of the GCL WRC, the unimodal fitting curve overestimated the water content in the low-suction range where the geotextile pores and structure play a prominent role.

The inadequacy of using unimodal fitting curves to describe the full WRC of a GCL on the wetting path can be further illustrated using the complete water retention experimental data set reported by Lau et al. (2022a) as an example. The data set from 0.01 to 10^6 kPa on the wetting path are shown in Fig. 4. The data indicate that the GCLs exhibit a bimodal behavior on the wetting path where two distinct slopes can be identified around 1,000 kPa and in the low-suction range around 0.1–0.3 kPa for GCL1 and GCL2, and at slightly higher suctions for GCL3, GCL4, and GCL5, indicating a rapid increase in water content with decreasing suction. Both data sets were fitted and compared using the three aforementioned models, as shown in Fig. 4. Details of the curve fitting analysis are tabulated in Table 3.

The curve fitting was conducted by targeting a fit with the least residual sum of squares value. Subsequently, the corresponding goodness of fit, R^2, was used as the point of comparison between the models to evaluate their comparative reliability in estimating the water retention behavior of the GCL based on the given experimental data set. The analysis indicated that the R^2 values were improved in the order of vG model < FX model < Lu model. Nonetheless, the curve-fitting results using the three unimodal fitting equations on a bimodal data set were unsurprisingly inadequate. The reasonable statistical fit obtained misrepresents the actual observable data because the area between the data range of 0.2 to 2,000 kPa equals out on both sides of the fitted model. There are many data points anchoring the fit in the very-low-suction range.

For the GCLs, the vG and FX models tended to underestimate the water content at the slope around 100–3,000 kPa, which depicts bentonite capillary water. Furthermore, they also overestimated the water content in the lower suction range (0.1–50 kPa) because it trends toward the measured saturated water content parameter. Comparatively, the Lu (2016) model has a better fit overall, albeit still not fully capturing the water retention behavior in the 1–1,000 kPa region. Furthermore, it is difficult to derive any relevant physical interpretations from the fitted parameters of these models given in Table 3 for this analysis that could explain the GCLs' water retention behavior. Therefore, it is proposed that

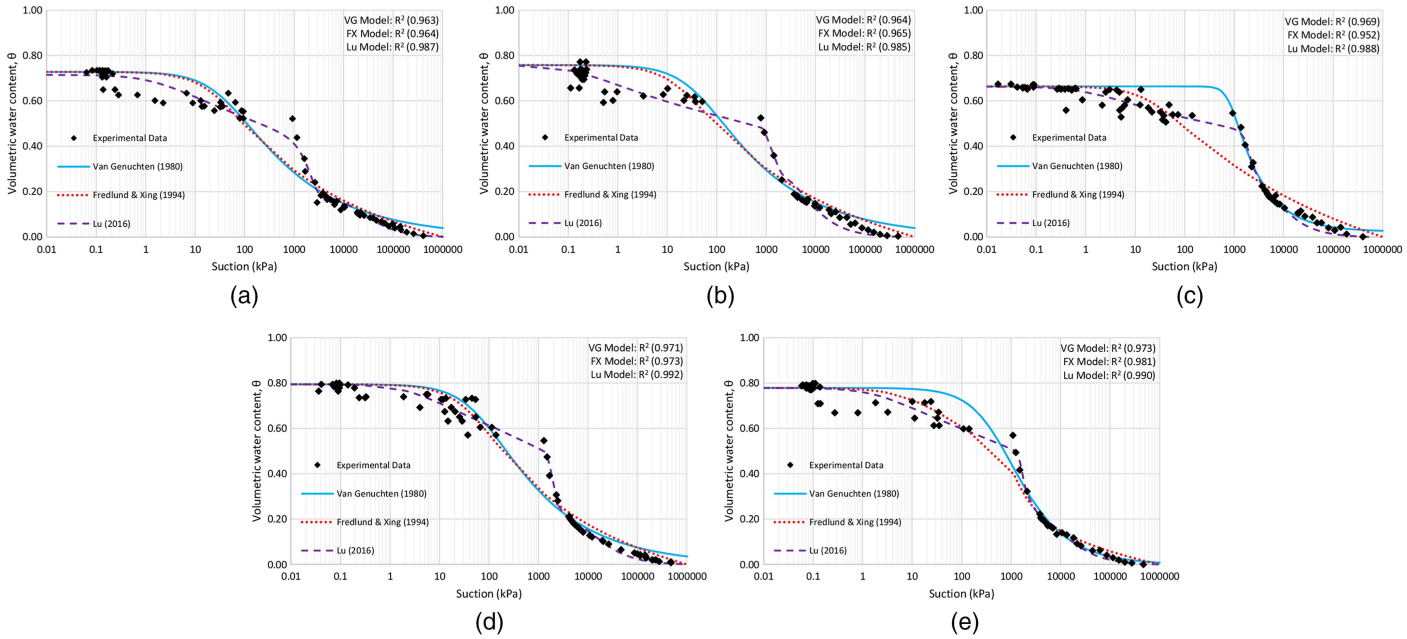

Fig. 4. Fitted curves of the experimental data across the full suction range (0.1–10^6 kPa): (a) GCL1; (b) GCL2; (c) GCL3; (d) GCL4; and (e) GCL5.

© ASCE

Table 3. Summary of the curve-fitting process of the various WRC models on the different GCL data sets

Data set	Fitted data suction range	Fitting model	$\theta_{a\max}/\theta_r$	ψ_c/ψ_r (kPa)	a ($\alpha = 1/a$) (kPa)	n	m	$\Psi_{\max}$ (kPa)	All ψ R^2	$\psi > 1$ MPa R^2
GCL1	All data (0.01–10^6 kPa)	Van Genuchten (1980)	0.000	—	39	1.100	0.262	—	0.962	0.880
		Fredlund and Xing (1994)	—	352	24	1.100	0.507	1,000,000	0.964	0.833
		Lu (2016)	0.169	1,877	2	1.100	0.019	1,200,000	0.987	0.950
	>1 MPa data (10^3–10^6 kPa)	Van Genuchten (1980)	0.041	—	528	10.000	0.075	—	—	0.960
		Fredlund and Xing (1994)	—	22,774	772	4.475	0.671	1,000,000	—	0.984
		Lu (2016)	0.133	10,859	926	2.821	0.032	1,200,000	—	0.984
	All data (0.01–10^6 kPa)	Proposed fitting equation — Bentonite component	0.147	12,982	1,270	3.491	0.026	1,200,000	0.994	0.982
		Proposed fitting equation — GTX component	—	5	0.25	10.000	—	—		
GCL2	All data (0.01–10^6 kPa)	Van Genuchten (1980)	0.000	—	41	1.100	0.266	—	0.964	0.936
		Fredlund and Xing (1994)	—	350	17	1.100	0.489	1,000,000	0.964	0.879
		Lu (2016)	0.300	1,315	0.13	1.100	0.010	545,210	0.985	0.958
	>1 MPa data (10^3–10^6 kPa)	Van Genuchten (1980)	0.011	—	368	10.000	0.056	—	—	0.978
		Fredlund and Xing (1994)	—	10,605	585	3.004	0.738	1,000,000	—	0.991
		Lu (2016)	0.133	12,571	710	2.423	0.081	489,561	—	0.997
	All data (0.01–10^6 kPa)	Proposed fitting equation — Bentonite component	0.146	10,232	1,026	2.869	0.050	643,547	0.994	0.997
		Proposed fitting equation — GTX component	—	28	0.23	2.852	—	—		
GCL3	All data (0.01–10^6 kPa)	Van Genuchten (1980)	0.023	—	819	4.023	0.180	—	0.969	0.984
		Fredlund and Xing (1994)	—	425	22	1.100	0.398	1,000,000	0.952	0.837
		Lu (2016)	0.300	2,041	1	1.100	0.010	544,892	0.988	0.967
	>1 MPa data (10^3–10^6 kPa)	Van Genuchten (1980)	0.023	—	814	4.196	0.171	—	—	0.984
		Fredlund and Xing (1994)	—	8,401	1,000	2.780	0.749	1,000,000	—	0.991
		Lu (2016)	0.118	11,024	1,334	2.543	0.096	502,724	—	0.995
	All data (0.01–10^6 kPa)	Proposed fitting equation — Bentonite component	0.151	8,411	1,962	3.574	0.024	1,197,457	0.990	0.991
		Proposed fitting equation — GTX component	—	288	0.72	1.388	—	—		
GCL4	All data 0.01–10^6 kPa)	Van Genuchten (1980)	0.000	—	66	1.100	0.293	—	0.971	0.905
		Fredlund and Xing (1994)	—	560	38	1.100	0.554	1,000,000	0.973	0.851
		Lu (2016)	0.199	2,047	3	1.100	0.011	1,200,000	0.992	0.984
	>1 MPa data (10^3–10^6 kPa)	Van Genuchten (1980)	0.021	—	710	10.000	0.078	—	—	0.985
		Fredlund and Xing (1994)	—	8,939	1,000	4.177	0.714	1,000,000	—	0.998
		Lu (2016)	0.132	9,516	1,180	2.807	0.032	1,200,000	—	0.995
	All data (0.01–10^6 kPa)	Proposed fitting equation — Bentonite component	0.158	8,291	1,696	3.782	0.021	1,200,000	0.993	0.991
		Proposed fitting equation — GTX component	—	70	0.12	1.147	—	—		
GCL5	All data (0.01–10^6 kPa)	Van Genuchten (1980)	0.000	—	646	1.100	0.550	—	0.973	0.955
		Fredlund and Xing (1994)	—	8	926	3.318	0.354	1,000,000	0.981	0.970
		Lu (2016)	0.222	1,908	1,096	1.100	0.010	1,052,832	0.990	0.983
	>1 MPa data (10^3–10^6 kPa)	Van Genuchten (1980)	0.015	—	710	10.000	0.069	—	—	0.988
		Fredlund and Xing (1994)	—	3,970	1,000	3.755	0.670	1,000,000	—	0.996
		Lu (2016)	0.160	6,748	1,180	2.816	0.020	1,200,000	—	0.997
	All data (0.01–10^6 kPa)	Proposed fitting equation — Bentonite component	0.167	6,642	1,451	3.434	0.017	1,200,000	0.993	0.994
		Proposed fitting equation — GTX component	—	355	0.23	1.426	—	—		

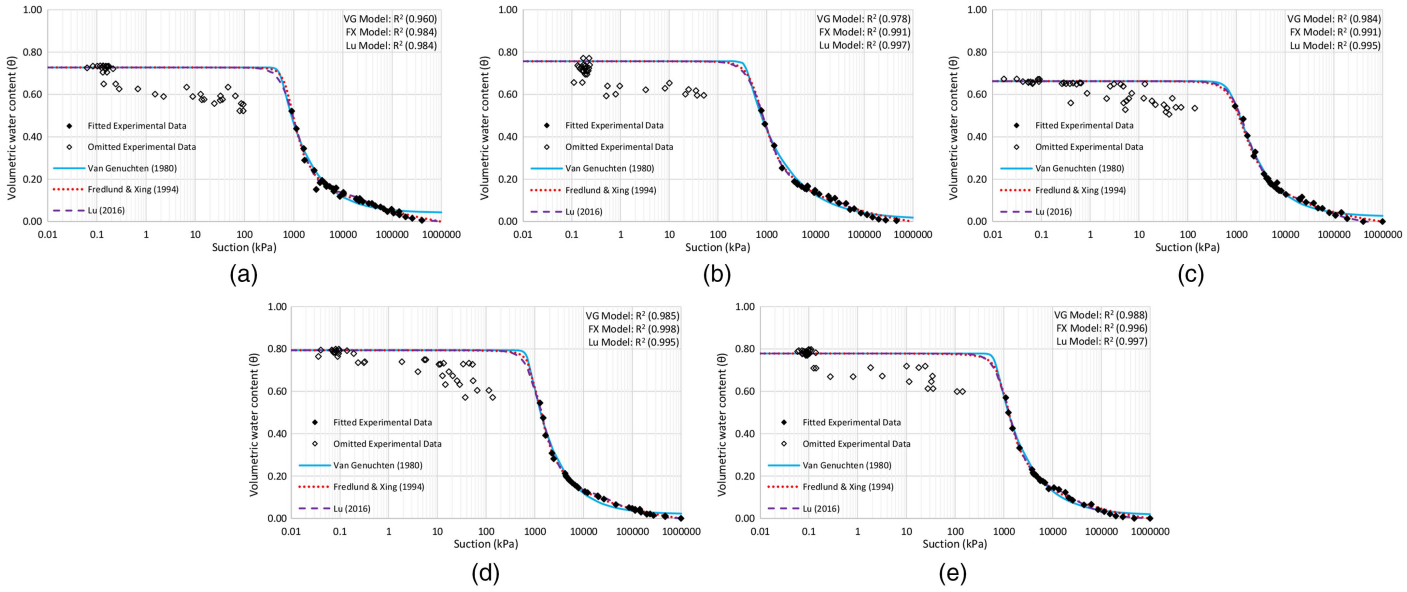

Fig. 5. Fitted curves of the experimental data from 10^3 to 10^6 kPa: (a) GCL1; (b) GCL2; (c) GCL3; (d) GCL4; and (e) GCL5.

although these models are appropriate at fitting GCL water retention behavior in the suction regions where the bentonite fraction is dominant (>1 MPa) as shown in literature, they are inadequate when considering the very-low-suction ranges (<100 kPa).

The curve-fitting analysis was repeated on a truncated variant of the same experimental data set where it was limited to the ranges where the bentonite fraction was dominant (around 10^3–10^6 kPa). The analysis is shown in Fig. 5 and tabulated in Table 3. When comparing the three fitting models, the Lu (2016) model provided the best fit for the GCLs. The vG model tended to deviate from the data, especially at suction >100 MPa, and the nature of the FX model forces it to terminate at the highest suction of 10^6 kPa. Another difference is that the Lu (2016) model can clearly distinguish between bentonite adsorption and capillary water on the wetting path, as shown in Fig. 5. These results reaffirm the notion that the model proposed by Lu (2016) provides clear insights into the water retention regimes of GCLs, especially in regions dominated by the bentonite pore series.

The performance of the three fitting models fared significantly better in this analysis than the models' performance for the data set spanning across the full suction ranges shown in Fig. 4. Furthermore, the fitted parameters, especially for Lu (2016) model, were more consistent with expected bentonite behavior. Nonetheless, the fitted curves for the truncated data set tended to overestimate the actual water content of the GCL on the wetting path in the suction ranges <100 kPa. This highlights that these unimodal fitting equations are adept at describing the water retention behavior of the bentonite component but, when fitted to a truncated data set, mask the known changes that occur in the very-low-suction region of the GCL. The statistical analysis depicted in Figs. 4 and 5 brings to light the importance of having a measured experimental data set that extends into the very-low-suction range (<1 kPa) as well as the inadequacy of these models at fitting the bimodal water retention behavior of the GCL when analyzing suction ranging from 0.1 to 10^6 kPa. Thus, when investigating the water retention curve of GCL across its broad spectrum of suctions, a bimodal general equation considering the water retention regime of both the geotextile and bentonite components will be more appropriate.

Proposed Modified WRC Model for GCLs

The proposed modified WRC model for GCLs aims to provide a closed-form continuous fitting equation that can depict the bimodal characteristics of the GCL and give fitting parameters physical interpretations that distinguish the various water retention regimes dictating GCL hydraulic behavior. The model presented by Lu (2016) has been proven to be thermodynamically rigorous and, as shown previously, suitable for characterizing the unimodal shape of the GCL bentonite component. However, the unimodal fitting equation will not suffice when describing bimodal water retention behavior. The proposed bimodal water retention model for GCLs expands on the Lu (2016) model and incorporates the water retention behavior observed at the low-suction ranges of the GCL.

There are three different approaches to developing equations for bimodal water retention curves. As characterized in literature, these approaches are the piecewise approach, the unique parameter approach, and the fraction of the total volume approach. Firstly, the piecewise method was disregarded because, despite its easiness in optimizing the fitting parameters in separate unimodal equations, it often required an arbitrarily determined intersection point to combine the two separate equations (Burger and Shackelford 2001). This leads to the issue of fitting parameters being nonunique.

The unique parameter approach is generally favored because it overcomes the problem of nonunique parameters, usually the by-product of the optimization process involving many fitted parameters, as in the case of a bimodal WRC equation. This is generally achieved by incorporating parameters that can be obtained graphically into the models to minimize the number of fitting parameters needed for the curve-fitting process (Gitirana and Fredlund 2004; Satyanaga et al. 2013; Li et al. 2014; Wijaya and Leong 2016). However, this is neither ideal nor practical for GCL WRCs due to the difficulty and complexity of measuring the GCLs' WRC across its entire suction range. Hence, it might not always be possible to determine graphically the necessary parameters required in this approach.

Therefore, the approach adopted for the proposed bimodal WRC equation is the fraction of the total volume approach. Under this approach, the estimated water content at a given suction is represented by the summation of both the macropore and micropore

fractions. The assumption is that the water content at full saturation can be expressed by the medium's total porosity, which is equal to the sum of all existing pore series (Zhang and Chen 2005). This can be expressed mathematically as follows:

$$w(\psi) = w_1 f_1(\psi) + w_2 f_2(\psi) \tag{5}$$

$$w_{\text{sat}} = w_1 + w_2 \tag{6}$$

where $w(\psi)$ = water content of the material at a given suction, ψ; w_{sat} = saturated water content of the material; w_1 and w_2 = water content of the various pore series (macropores and micropores) present in the system; and $f_1(\psi)$ and $f_2(\psi)$ = dimensionless WRC functions relating to the suction of the material.

By combining the expression of the various pores within a single equation, a smooth and continuous WRC can be produced to describe the bimodal behavior of the GCL. Furthermore, the model presented by Lu (2016), which forms the basis of this modified equation, was also established within the same theoretical framework, where the WRC was developed by distinguishing the total pore water volume into fractions describing adsorption and capillary water. Thus, to capture the bimodality of the GCL water retention behavior, the fraction of pore water as observed in the very-low-suction range must be incorporated into the WRC equation. The pore series in this suction range is believed to be dictated by the geotextiles and the GCL structure. It encompasses the pore water in the geotextiles and includes bentonite extrusion into the geotextile pores and, more significantly, the volume changes due to bentonite swelling from the geotextile fibers being pulled and stretched. The assumption is that these phenomena can be characterized as capillary water in the geotextile pores. Thus, the proposed general bimodal equation can be expressed

$$w(\psi) = w_{a,\text{bent}} f_1(\psi) + w_{c,\text{bent}} f_2(\psi) + w_{c,\text{gtx}} f_3(\psi) \tag{7}$$

$$w_{\text{sat}} = w_{a,\text{bent}} + w_{c,\text{bent}} + w_{c,\text{gtx}} \tag{8}$$

where w_{sat} = saturated water content/total porosity; $w_{a,\text{bent}}$ = maximum adsorption water of bentonite; $w_{c,\text{bent}}$ = capillary water of bentonite; $w_{c,\text{gtx}}$ = capillary water of the geotextiles; and $f_1(\psi)$, $f_2(\psi)$, and $f_3(\psi)$ = dimensionless WRC functions relating to the suction. The expression for the adsorption and capillary water of the bentonite was adapted from Lu (2016) as presented in Eqs. (3) and (4), respectively. The equation for capillary water in the geotextile regime also follows the capillary model in Lu (2016) that utilizes the cumulative distribution function to simulate the probability of water condensation. Thus, the WRC of the geotextile regime is expressed volumetrically as follows:

$$\theta_{c,\text{gtx}}(\psi) = [\theta_s - \theta_{a,\text{bent}}(\psi) - \theta_{c,\text{bent}}(\psi)] \times \frac{\left[1 - \text{erf}\left(\frac{\psi - \psi_{c,\text{gtx}}}{\sqrt{2}\sigma_{c,\text{gtx}}}\right)\right]}{2 \times [1 + (\alpha_{\text{gtx}}\psi)^p]^{1-\frac{1}{p}}} \tag{9}$$

where $\psi_{c,\text{gtx}}$ = mean cavitation suction for the geotextile regime; $\sigma_{c,\text{gtx}}$ =cavitation deviation for the geotextile regime proposed to be $0.5\psi_{c,\text{gtx}}$ (Herbert et al. 2006); α_{gtx} = parameter indicating the inverse of AExV for the geotextile regime; and p = parameter linked to the pore-size distribution of the geotextile regime.

Therefore, the proposed bimodal water retention equation for GCL can be defined by combining Eqs. (3), (4) and (9). It is written volumetrically as follows:

$$\theta(\psi) = \theta_{a,\text{bent}}(\psi) + \theta_{c,\text{bent}}(\psi) + \theta_{c,\text{gtx}}(\psi) \tag{10}$$

$$\begin{aligned}\theta(\psi) = \theta_{a\max}\left\{1 - \left[\exp\left(1 - \frac{\psi_{\max}}{\psi}\right)\right]^m\right\} + [\theta_{s,\text{bent}} - \theta_{a,\text{bent}}(\psi)] \\ \times \frac{[1 - \text{erf}(\frac{\psi - \psi_{c,\text{bent}}}{\sqrt{2}\sigma_{c,\text{bent}}})]}{2 \times [1 + (\alpha_{\text{bent}}\psi)^n]^{1-\frac{1}{n}}} + [\theta_s - \theta_{a,\text{bent}}(\psi) - \theta_{c,\text{bent}}(\psi)] \\ \times \frac{[1 - \text{erf}(\frac{\psi - \psi_{c,\text{gtx}}}{\sqrt{2}\sigma_{c,\text{gtx}}})]}{2 \times [1 + (\alpha_{\text{gtx}}\psi)^p]^{1-\frac{1}{p}}}\end{aligned} \tag{11}$$

where θ_s = measured saturated water content of the GCL; and $\theta_{s,\text{bent}}$ = saturated water content of the bentonite component at suction less than its air expulsion value. The proposed model's conceptual water retention curve is illustrated in Fig. 6, where the

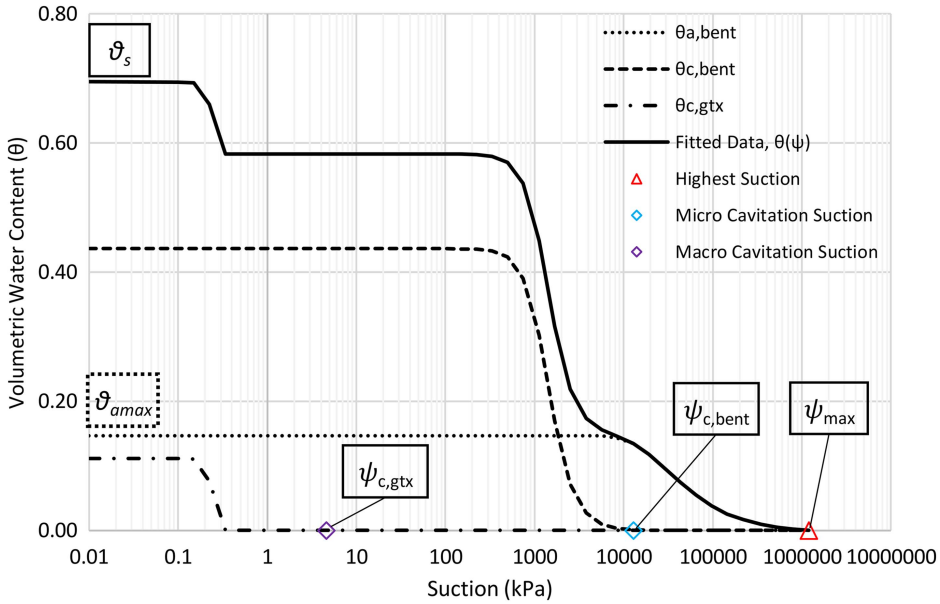

Fig. 6. Conceptual illustration of proposed WRC model for GCLs fitted with highlighted parameters.

key physical parameters are identified to describe the physical interpretations of the parameters used in the model.

Discussion

The performance of the proposed fitting curve equation at predicting the GCL water retention behavior was assessed by employing it on the experimental data sets of five different GCLs reported by Lau et al. (2022a). The optimization process was conducted on the measured data set expressed in volumetric water content.

Comparison between Existing and Proposed Models

Comparisons were made with models typically used to curve fit measured GCL data sets. The efficacy of each model was evaluated statistically based on the corresponding goodness of fit (R^2) for both the region covering the bentonite region (>1 MPa) and the full suction range. The comparisons among the four models, namely vG, FX, Lu (2016), and the new proposed water retention model are illustrated both volumetrically and gravimetrically in Fig. 7. The analysis results and relevant fitted parameters are detailed in Table 3.

As observed in Fig. 7 and Table 3, the curve-fitting analysis results indicated that the proposed WRC model provides a better fit for various GCLs than the other models (Table 3). The proposed model's statistical fit across the entire suction range was consistently the highest in all data sets of the five different GCLs. For a powdered bentonite GCL with low polymer loading like GCL1, the proposed model ($R^2 = 0.994$) showed an improved fitting from the other models ($R^2 = 0.962$–0.987). For an unmodified granular bentonite GCL like GCL2, the proposed model ($R^2 = 0.994$) provided a better fitting than the other models ($R^2 = 0.964$–0.985). Similarly, the proposed model also has the highest R^2 for granular bentonite GCLs with high polymer loading like GCL3 ($R^2 = 0.990$ versus $R^2 = 0.952$–0.988), GCL4 ($R^2 = 0.993$ versus $R^2 = 0.971$–0.992), and GCL5 ($R^2 = 0.993$ versus $R^2 = 0.973$–0.990). This is unsurprising because the improved fit of the proposed model can be observed visually from the graphs shown in Fig. 7. As mentioned previously, the FX and vG models overestimate the water retention behavior in the low-suction range (around 1 kPa). The proposed model adequately describes both the water retention behavior in the low-suction range (around 1 kPa) and the bentonite capillary region (around 1 MPa) characterized by the steep water content increase when fitted to the full suction range, including an additional component in its model that recognizes the dominant geotextile regime.

Furthermore, because the Lu (2016) model is adept at describing the GCL behavior at higher suction ranges when only analyzing suctions >1 MPa (Fig. 5), the proposed model captures water retention behavior at high suctions, similar to the Lu (2016) model, without being affected by its ability to fit low-suction data. In this analysis, the proposed model's performance was significantly better than the other models at suctions >1 MPa when fitted to the full suction range data for all five GCLs (Table 3).

Finally, the performance of the proposed model was also compared with the models that were fitted to data where suction was >1 MPa. The Lu (2016) model was chosen over the FX and vG models for direct comparison with the proposed model at high-suction ranges (>1 MPa) because it distinguishes capillary and adsorption water, as well as typically has the best fit across the five different GCLs among the three unimodal equations. The comparison between the proposed model and the Lu (2016) model revealed that both models yielded similar R^2 for suctions >1 MPa (Table 3).

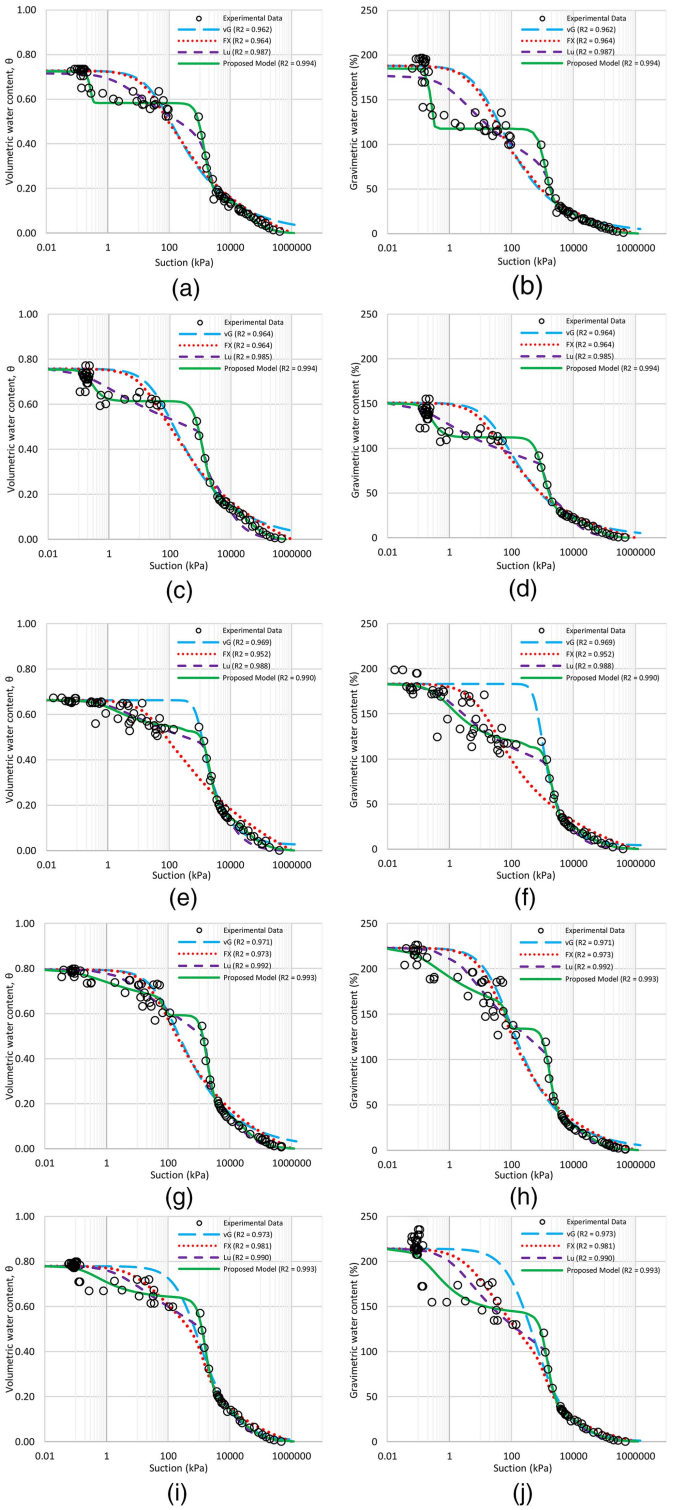

Fig. 7. Comparison of the various fitting models on five different GCL water retention data sets: (a and b) GCL1; (c and d) GCL2; (e and f) GCL3; (g and h) GCL4; and (i and j) GCL5.

Additionally, the fitted parameters yielded from the proposed model for the bentonite component were similar to the parameters generated by Lu (2016) when fitted to data with suction >1 MPa. This indicates that the proposed model can adequately capture the high-suction (bentonite component) behavior of the GCL and is not affected by including the geotextile component in the model.

Thus, the uncertainty present in the data collection is greater than that of the proposed model and is the main limitation to the data best fit rather than the model performance.

Another issue with the unimodal models when fitting a full suction range data is that there is a possibility that the resulting fitted parameters lose their physical interpretation. This was prevalent even for the Lu (2016) model, despite yielding relatively high R^2 (0.985–0.992) for all five GCLs across the entire suction range. In this case, the Lu (2016) model yielded α (inverse of AExV, $1/\alpha$) parameters that were considered too high to describe the AExV of the bentonite component yet too low to be the AExV of the geotextile region. The fitted cavitation suction (ψ_c) parameter was generally too low to describe the cavitation point (condensation point in the case of the wetting path) of the bentonite component but too high to depict cavitation in the geotextile pores. This is the consequence of the models having to accommodate the data set's bimodality once measurements at the low-suction ranges are included.

The proposed model overcomes these limitations by modifying the Lu (2016) model to include the component that addresses the low-suction geotextile dominant regime. The proposed model distinguishes the behavior occurring at both high- and low-suction ranges, yielding unique parameters that adequately describe the water retention behavior across these suction regimes. This is reflected in the fitted parameters produced by the proposed model, which were dichotomized into the bentonite and geotextile components. The yielded parameters were within the ranges expected for both components. Additionally, the parameters produced by the proposed model in the bentonite component were compared with and validated by the parameters yielded by the Lu (2016) model fitted to only the high-suction data (Table 3).

Discussions on the Proposed Model

Fig. 8 illustrates the proposed models optimized to the measured data sets of the GCLs. In these figures, the solid line depicts the fitted curve, the dashed line represents the bentonite capillary regime ($\theta_{c,\text{bent}}$), the dotted line represents the bentonite adsorption regime ($\theta_{a,\text{bent}}$), the dashed and dotted lines represent the geotextile capillary regime ($\theta_{c,\text{gtx}}$), the darker diamond marker indicates the onset of the geotextile regime, the lighter diamond marker signifies the cavitation suction for the bentonite regime, and the triangle marker represents the highest suction for the material. As previously discussed, the overall shape of the GCL WRC is bimodal on the wetting path. It was observed in Fig. 1(a) that across all five different GCL products, the shape of the initial wetting path was primarily the same at high suction. It only started diverging when it reached the bentonite capillary regime, where the GCLs with higher polymer loading began attracting more water at higher suctions. The differences between the water retention behavior of the GCLs become more apparent in the low-suction range (geotextile regime), where there is a larger scatter of data. These differences stem from a combination of the GCLs having different geotextile construction, the type of polymer used, if any, and its polymer loading. This reaffirms the importance of having a measured experimental data set extending into the very-low-suction ranges (<1 kPa).

From the fitted curves, the shape of the WRC in the geotextile regime was observed to be different depending on the polymer loading of the GCL. The slope in the low-suction range was steeper and more distinct for GCLs with no or low polymer enhancement like GCL1 and GCL2, whereas for GCLs with high polymer loadings like GCL3, GCL4, and GCL5, the slope was less distinct and spanned across a wider range of suctions. This can be attributed to the fact that the GCLs with higher polymer loading have a larger polymer fraction with a higher adsorption capacity that attracts more water into the GCL. This causes higher bentonite swelling in the GCL (also indicated by the higher swell index of bentonite with higher polymer loading), activating and challenging the geotextile fibers. This means that the onset of the geotextile regime would occur at higher suctions than GCLs with no or low polymer loading.

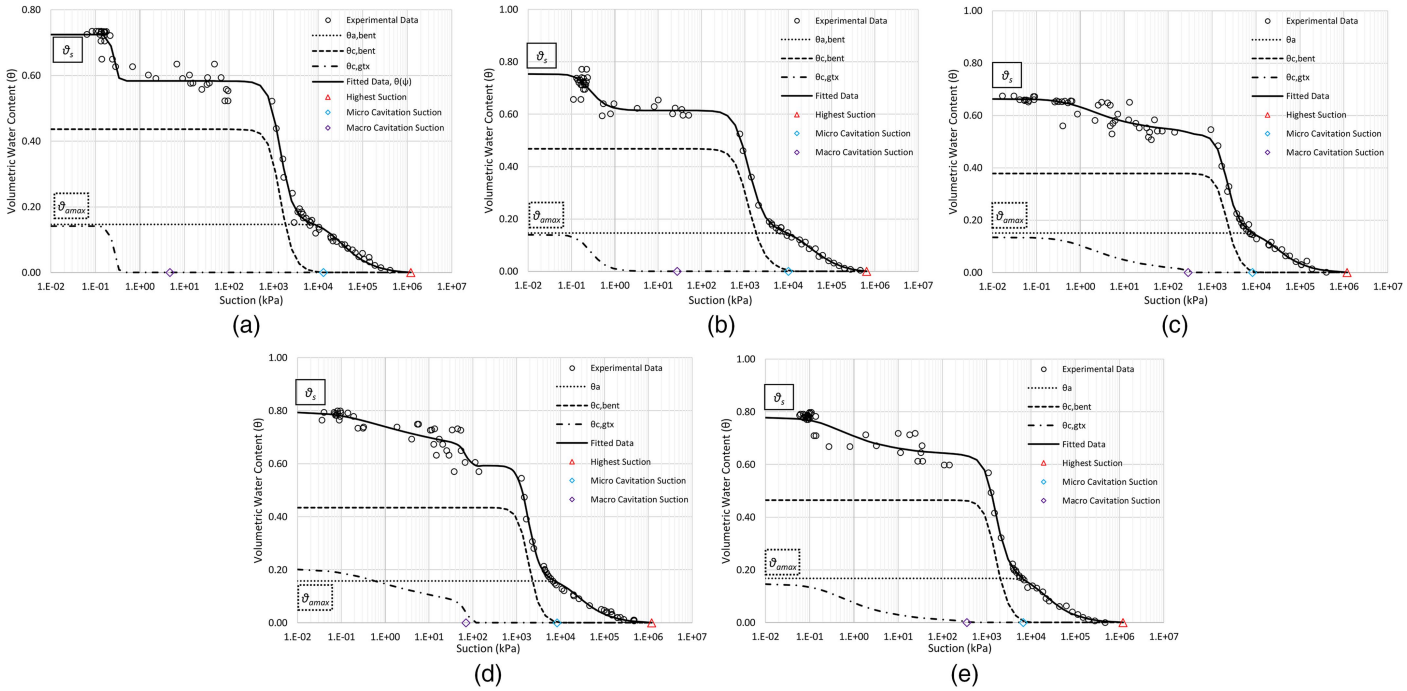

Fig. 8. Fitted WRC of the proposed model optimized to the measured experimental data set: (a) GCL1; (b) GCL2; (c) GCL3; (d) GCL4; and (e) GCL5.

This is supported by the fitted cavitation suction parameter ($\psi_{c,gtx}$) yielded in this analysis, indicating the onset of the geotextile regime. GCL1 and GCL2 yielded $\psi_{c,gtx} = 5$ and 28 kPa, respectively, which are lower than the values for high-polymer-loading GCLs like GCL3 ($\psi_{c,gtx} = 288$ kPa), GCL4 ($\psi_{c,gtx} = 70$ kPa), and GCL5 ($\psi_{c,gtx} = 355$ kPa). This shows that for GCL1 and GCL2 (no or low polymer loading), the GTX dominates this range and starts wetting at <30 kPa. However, the presence of higher polymer loading in GCL3, GCL4, and GCL5 allows this feature to extend and initiate wetting at much higher suctions. Importantly, the AExV ($1/\alpha$) values in the geotextile regime yielded by the proposed model for the GCLs ranged between 0.12 and 0.72 kPa. These values are consistent with the AExV reported for geotextiles (Bouazza et al. 2006a; Nahlawi et al. 2007).

Lastly, the fitted parameter p, which controls the shape of the WRC in the geotextile regime, was lower for the GCLs with higher polymer loading ($p = 1.147$–1.426) when compared with GCL1 ($p = 10$) and GCL2 ($p = 2.852$). A lower p-value describes a more gradual slope spanning a larger suction range, as observed for GCL3, GCL4, and GCL5, whereas a higher p-value indicates a steeper slope, seen in the fitted curves for GCL1 and GCL2.

In the bentonite capillary regime, the AExV for the high-polymer GCLs ranged from 1,451 to 1,962 kPa. It is higher than the AExV for GCL1 ($a = 1{,}270$ kPa) and GCL2 ($a = 1{,}026$ kPa). This is due to the higher polymer fraction (or possibly a different polymer type), which has a higher adsorption capacity that allows these GCLs to attract water more easily, thus achieving a state where the air is expelled from the bentonite at a higher suction. On the other hand, the cavitation suction ($\psi_{c,bent}$) for the GCLs fell within similar suction ranges. The GCLs with high polymer loading had smaller $\psi_{c,bent}$ values (6,642–8,411 kPa) than the other two GCLs (10,232–12,982 kPa). However, these differences are marginal within the current context, which is unsurprising because these GCLs tended to behave similarly at the high-suction range, predominantly because the bentonite fraction controls the behavior in this range. Furthermore, the total adsorption capacity (θ_{amax}) of the GCLs was found to be within the range of 0.146–0.167. This is consistent with the θ_{amax} values obtained by Lu (2016) for Denver bentonite (0.159) and Wyoming bentonite (0.192). This supports the notion that different GCLs behave similarly at the high-suction range and are dominated by the bentonite component.

Limitations

The proposed model describes the wetting path of the GCL (utilizing measured data of GCLs undergoing the wetting process) and, as such, does not capture the drying path behavior of GCLs. The drying path behavior must consider hysteresis, structural changes due to excessive bentonite swelling during the wetting process, and even possible polymer elution. Furthermore, a challenge with the increased number of parameters in this proposed model is the possibility of failure during the curve-fitting process (i.e., the model generates unrealistic fitting parameter values). Thus, lower and upper bounds were applied to some parameters to aid the optimization process during curve fitting. This ensures that the parameters are unique and maintain physical significance. These parameter boundaries are listed in Table 4.

Conclusions

The existing fitting equations typically used for GCLs like the vG and FX models are appropriate for fitting the GCL WRC in the suction ranges where bentonite fraction is dominant (>1 MPa). However, they are inadequate at describing the bimodal data when considering the full suction range of the GCL (10^{-2}–10^{6} kPa). They tend to underestimate the water content around 100–3,000 kPa, which depicts the bentonite capillary water, and overestimate the water content in the lower-suction range (0.1–50 kPa) because it trends toward the measured saturated water content parameter. Comparatively, the Lu (2016) model had a better overall fit, although it still does not fully capture the water retention behavior in the 1–1,000-kPa region. Consequently, it is difficult to derive any relevant physical interpretations from these models' fitted parameters to explain the GCLs' water retention behavior.

A new bimodal WRC equation for GCLs was proposed in this paper to address the bimodality of the measured GCL WRC data on the wetting path. The proposed model is a closed-form continuous fitting equation that depicts the bimodal characteristics of the GCL and yields fitting parameters with physical interpretations that distinguish the critical water retention regimes dictating GCL hydraulic behavior. It is an extension of the Lu (2016) model's concepts with the addition of the water retention mechanism in the low-suction range depicting the geotextile capillary regime. The pore water fraction in the geotextile capillary regime was incorporated by adopting the total volume approach. It describes the pore water in the geotextiles, any bentonite extrusion into the geotextile pores, and, more significantly, additional volume changes due to bentonite swelling from the geotextile fibers being stretched.

The proposed WRC model is characterized as the sum of its bentonite adsorption water ($\theta_{a,bent}$), bentonite capillary water ($\theta_{c,bent}$), and geotextile capillary water ($\theta_{c,gtx}$). The bentonite adsorption water is defined as the parameter depicting its total adsorption capacity (θ_{amax}), along with the adsorption strength parameter (m) and its highest suction (ψ_{max}). The bentonite capillary water was formulated based on the cumulative distribution function for cavitation. It is described using four parameters, namely the bentonite cavitation suction ($\psi_{c,bent}$), the bentonite AExV(α_{bent}), the parameter linked to pore size distribution (n), and the saturated water content for the bentonite component in the GCL ($\theta_{s,bent}$). The geotextile capillary water was also defined using the same concept as bentonite capillary water but using different parameters ($\psi_{c,gtx}$, α_{gtx}, p, and θ_s). Therefore, the proposed model combines all the stated parameters to provide a continuous curve describing the bimodal behavior of the GCL WRC.

The proposed model's performance was assessed and compared using a statistical analysis based on its least-squares fit expressed as the models' coefficient of determination (R^2). The proposed model provided the best fit over the entire suction and at high suction (>1 MPa). The Lu (2016) model was employed to fit the data sets with suctions larger than 1 MPa to capture the bentonite component's water retention behavior (high-suction range) of the GCL. The proposed model was compared with it and was observed to yield a comparable R^2 and similar fitted parameters. This indicates that the proposed model can capture the high-suction (bentonite component) behavior of the GCL and is not affected by the

Table 4. Lower and upper boundaries of the curve fitting parameters

Boundary	θ_{amax}	$\psi_{c,bent}$ (kPa)	$\psi_{c,gtx}$ (kPa)	α_{bent} (kPa^{-1})	α_{gtx} (kPa^{-1})	n	p	m	ψ_{max} (kPa)
Lower	0.01	1,000	0.1	0.0001	1	1.1	1.1	0.01	—
Upper	0.30	25,000	1,000	0.1	10	10	10	1.00	1.2×10^6

geotextile fraction in the model. The GCL WRCs were broadly similar at high-suction ranges. Their behavior started diverging beyond the bentonite capillary regime, where their shape in the geotextile regime hinged upon various factors like polymer type, polymer loading, and GCL structure. The proposed model is adequate at predicting the water retention behavior of the GCL across the full suction range on the wetting path.

Data Availability Statement

Some or all data, models, or code that support the findings of this study are available from the corresponding author upon reasonable request.

Acknowledgments

This research project was supported by the Australian Research Council's Discovery Projects funding scheme (Project No. DP190103682). This support is gratefully acknowledged.

References

Abuel-Naga, H., and A. Bouazza. 2010. "A novel laboratory technique to determine the water retention curve of geosynthetic clay liners." *Geosynth. Int.* 17 (5): 313–322. https://doi.org/10.1680/gein.2010.17.5.313.

Acikel, A. S., A. Bouazza, W. P. Gates, R. M. Singh, and R. K. Rowe. 2020. "A novel transient gravimetric monitoring technique implemented to GCL osmotic suction control." *Geotext. Geomembr.* 48 (6): 755–767. https://doi.org/10.1016/j.geotexmem.2020.05.002.

Acikel, A. S., A. Bouazza, R. M. Singh, W. P. Gates, and R. K. Rowe. 2022. "Challenges of the filter paper suction measurements in geosynthetic clay liners: Effects of method, time, capillarity, and hysteresis." *Geotech. Test. J.* 45 (2): 449–467. https://doi.org/10.1520/GTJ20200168.

Acikel, A. S., W. P. Gates, R. M. Singh, A. Bouazza, D. G. Fredlund, and R. K. Rowe. 2018a. "Time-dependent unsaturated behaviour of geosynthetic clay liners." *Can. Geotech. J.* 55 (12): 1824–1836. https://doi.org/10.1139/cgj-2017-0646.

Acikel, A. S., W. P. Gates, R. M. Singh, A. Bouazza, and R. K. Rowe. 2018b. "Insufficient initial hydration of GCLs from some subgrades: Factors and causes." *Geotext. Geomembr.* 46 (6): 770–781. https://doi.org/10.1016/j.geotexmem.2018.06.007.

Alonso, E. E., J. Vaunat, and A. Gens. 1999. "Modelling the mechanical behaviour of expansive clays." *Eng. Geol.* 54 (1–2): 173–183. https://doi.org/10.1016/S0013-7952(99)00079-4.

Anderson, R., M. T. Rayhani, and R. K. Rowe. 2012. "Laboratory investigation of GCL hydration from clayey sand subsoil." *Geotext. Geomembr.* 31 (Apr): 31–38. https://doi.org/10.1016/j.geotexmem.2011.10.005.

ASTM. 2016. *Standard test method for fluid loss of clay component of geosynthetic clay liners*. ASTM D5891. West Conshohocken, PA: ASTM.

ASTM. 2018a. *Standard test method for measuring mass per unit of geosynthetic clay liners*. ASTM D5993. West Conshohocken, PA: ASTM.

ASTM. 2018b. *Standard test method for swell index of clay mineral component of geosynthetic clay liners*. ASTM D5890. West Conshohocken, PA: ASTM.

ASTM. 2020. *Standard test method for determining average bonding peel strength between top and bottom layers of needle-punched geosynthetic clay liners*. ASTM D6496. West Conshohocken, PA: ASTM.

Barclay, A., and M. T. Rayhani. 2013. "Effect of temperature on hydration of geosynthetic clay liners in landfills." *Waste Manage. Res.* 31 (3): 265–272. https://doi.org/10.1177/0734242X12471153.

Battaglia, S., L. Leoni, and F. Sartori. 2006. "A method for determining the CEC and chemical composition of clays via XRF." *Clay Miner.* 41 (3): 717–725. https://doi.org/10.1180/0009855064130214.

Beddoe, R. A., W. A. Take, and R. K. Rowe. 2011. "Water-retention behavior of geosynthetic clay liners." *J. Geotech. Geoenviron. Eng.* 137 (11): 1028–1038. https://doi.org/10.1061/(ASCE)GT.1943-5606.0000526.

Bouazza, A. 2002. "Geosynthetic clay liners." *Geotext. Geomembr.* 20 (1): 3–17. https://doi.org/10.1016/S0266-1144(01)00025-5.

Bouazza, A. 2021. "Interaction between PFASs and geosynthetic liners: Current status and the way forward." *Geosynth. Int.* 28 (2): 214–223. https://doi.org/10.1680/jgein.20.00033.

Bouazza, A., M. A. Ali, W. P. Gates, and R. K. Rowe. 2017a. "New insight on geosynthetic clay liner hydration: The key role of subsoils mineralogy." *Geosynth. Int.* 24 (2): 139–150. https://doi.org/10.1680/jgein.16.00022.

Bouazza, A., M. A. Ali, R. K. Rowe, W. P. Gates, and A. El-Zein. 2017b. "Heat mitigation in geosynthetic composite liners exposed to elevated temperatures." *Geotext. Geomembr.* 45 (5): 406–417. https://doi.org/10.1016/j.geotexmem.2017.05.004.

Bouazza, A., and J. J. Bowders. 2010. *Geosynthetic clay liners for waste containment facilities*. London: CRC Press.

Bouazza, A., M. Freund, and H. Nahlawi. 2006a. "Water retention of nonwoven polyester geotextiles." *Polym. Test.* 25 (8): 1038–1043. https://doi.org/10.1016/j.polymertesting.2006.07.002.

Bouazza, A., and W. P. Gates. 2014. "Overview of performance compatibility issues of GCLs with respect to leachates of extreme chemistry." *Geosynth. Int.* 21 (2): 151–167. https://doi.org/10.1680/gein.14.00006.

Bouazza, A., and M. A. Rouf. 2021. "Hysteresis of the water retention curves of geosynthetic clay liners in the high suction range." *Geotext. Geomembr.* 49 (4): 1079–1084. https://doi.org/10.1016/j.geotexmem.2021.03.002.

Bouazza, A., M. A. Rouf, R. M. Singh, R. K. Rowe, and W. P. Gates. 2017c. "Gas advection-diffusion in geosynthetic clay liners with powder and granular bentonites." *Geosynth. Int.* 24 (6): 607–614. https://doi.org/10.1680/jgein.17.00027.

Bouazza, A., R. M. Singh, R. K. Rowe, and F. Gassner. 2014. "Heat and moisture migration in a geomembrane–GCL composite liner subjected to high temperatures and low vertical stresses." *Geotext. Geomembr.* 42 (5): 555–563. https://doi.org/10.1016/j.geotexmem.2014.08.002.

Bouazza, A., J. G. Zornberg, J. S. McCartney, and H. Nahlawi. 2006b. "Significance of unsaturated behaviour of geotextiles in earthen structures." *Aust. Geomech. J.* 41 (3): 133–142.

Bradshaw, S. L., C. H. Benson, and J. Scalia IV. 2013. "Hydration and cation exchange during subgrade hydration and effect on hydraulic conductivity of geosynthetic clay liners." *J. Geotech. Geoenviron. Eng.* 139 (4): 526–538. https://doi.org/10.1061/(ASCE)GT.1943-5606.0000793.

Burger, C. A., and C. D. Shackelford. 2001. "Evaluating dual porosity of pelletised diatomaceous earth using bimodal soil-water characteristic curve functions." *Can. Geotech. J.* 38 (1): 53–66. https://doi.org/10.1139/t00-084.

Carnero-Guzman, G. G., A. Bouazza, W. P. Gates, R. K. Rowe, and R. McWatters. 2021. "Hydration/dehydration behaviour of geosynthetic clay liners in the Antarctic environment." *Geotext. Geomembr.* 49 (1): 196–209. https://doi.org/10.1016/j.geotexmem.2020.10.020.

Carnero-Guzman, G. G., W. P. Gates, A. Bouazza, L. P. Aldridge, and H. N. Bordallo. 2019. "Using neutron spectroscopy to measure soil-water retention at high suction ranges." *Can. Geotech. J.* 56 (12): 1999–2003. https://doi.org/10.1139/cgj-2017-0718.

Chen, J., H. Salihoglu, C. H. Benson, W. J. Likos, and T. B. Edil. 2019. "Hydraulic conductivity of bentonite–polymer composite geosynthetic clay liners permeated with coal combustion product leachates." *J. Geotech. Geoenviron. Eng.* 145 (9): 04019038. https://doi.org/10.1061/(ASCE)GT.1943-5606.0002105.

Chevrier, B., D. Cazaux, G. Didier, M. Gamet, and D. Guyonnet. 2012. "Influence of subgrade, temperature and confining pressure on GCL hydration." *Geotext. Geomembr.* 33 (Aug): 1–6. https://doi.org/10.1016/j.geotexmem.2012.02.003.

Cui, Y. J. 2017. "On the hydro-mechanical behaviour of MX80 bentonite-based materials." *J. Rock Mech. Geotech. Eng.* 9 (3): 565–574. https://doi.org/10.1016/j.jrmge.2016.09.003.

Daniel, D. E. 1993. "Effects of partial wetting on the performance of the bentonite component of a geosynthetic clay liner."

In *Geosynthetics' 93*, 1482–1496. Roseville, MN: Industrial Fabrics Association International.
Delage, P. 2007. "Microstructure features in the behaviour of engineered barriers for nuclear waste disposal." In *Experimental unsaturated soil mechanics*, 11–32. Berlin: Springer.
Fehervari, A., W. P. Gates, A. Bouazza, and C. D. Shackelford. 2019. "Assessment of Bentonite compatibility with salinity using centrifugation-based water retention." *Geotech. Test. J.* 42 (2): 275–295. https://doi.org/10.1520/GTJ20170207.
Fredlund, D. G., and A. Xing. 1994. "Equations for the soil-water characteristic curve." *Can. Geotech. J.* 31 (4): 521–532. https://doi.org/10.1139/t94-061.
Frydman, S., and R. Baker. 2009. "Theoretical soil-water characteristic curves based on adsorption, cavitation, and a double porosity model." *Int. J. Geomech.* 9 (6): 250–257. https://doi.org/10.1061/(ASCE)1532-3641(2009)9:6(250).
Gates, W. P., et al. 2021. "Neutron scattering quantification of unfrozen pore water in frozen mud." *Microporous Mesoporous Mater.* 324 (Sep): 111267. https://doi.org/10.1016/j.micromeso.2021.111267.
Gates, W. P., G. Dumadah, and A. Bouazza. 2018. "Micro X-ray visualisation of the interaction of geosynthetic clay liner components after partial hydration." *Geotext. Geomembr.* 46 (6): 739–747. https://doi.org/10.1016/j.geotexmem.2018.07.006.
Gates, W. P., A. MacLeod, A. Fehervari, A. Bouazza, D. Gibbs, R. Hackney, D. L. Callahan, and M. Watts. 2020. "Interactions of per- and polyfluoralkyl substances (PFAS) with landfill liners." *Adv. Environ. Eng. Res.* 1 (4): 1. https://doi.org/10.21926/aeer.2004007.
Gens, A., and E. E. Alonso. 1992. "A framework for the behaviour of unsaturated expansive clays." *Can. Geotech. J.* 29 (6): 1013–1032. https://doi.org/10.1139/t92-120.
Ghavam-Nasiri, A., A. El-Zein, D. Airey, R. K. Rowe, and A. Bouazza. 2020. "Thermal desiccation of geosynthetic clay liners under brine pond conditions." *Geosynth. Int.* 27 (6): 593–605. https://doi.org/10.1680/jgein.20.00020.
Gitirana, G. F. N., and D. G. Fredlund. 2004. "Soil-water characteristic curve equation with independent properties." *J. Geotech. Geoenviron. Eng.* 130 (2): 209–212. https://doi.org/10.1061/(ASCE)1090-0241(2004)130:2(209).
Grim, R. E. 1968. *Clay mineralogy.* 2nd ed. New York: McGraw-Hill.
Herbert, E., S. Balibar, and F. Caupin. 2006. "Cavitation pressure in water." *Phys. Rev. E* 74 (4): 041603. https://doi.org/10.1103/PhysRevE.74.041603.
Hornsey, W. P., J. Scheirs, W. P. Gates, and A. Bouazza. 2010. "The impact of mining solutions/liquors on geosynthetics." *Geotext. Geomembr.* 28 (2): 191–198. https://doi.org/10.1016/j.geotexmem.2009.10.008.
Iryo, T., and R. K. Rowe. 2003. "On the hydraulic behavior of unsaturated nonwoven geotextiles." *Geotext. Geomembr.* 21 (6): 381–404. https://doi.org/10.1016/S0266-1144(03)00046-3.
Jensen, D. K., M. Tuller, L. W. de Jonge, E. Arthur, and P. Moldrup. 2015. "A new two-stage approach to predicting the soil water characteristic from saturation to oven-dryness." *J. Hydrol.* 521 (Feb): 498–507. https://doi.org/10.1016/j.jhydrol.2014.12.018.
Laird, D. A. 1996. "Model for crystalline swelling of 2: 1 phyllosilicates." *Clays Clay Miner.* 44 (4): 553–559. https://doi.org/10.1346/CCMN.1996.0440415.
Lau, Z. C., A. Bouazza, and W. P. Gates. 2022a. "Influence of polymer enhancement on water uptake, retention and barrier performance of geosynthetic clay liners." *Geotext. Geomembr.* 50 (4): 590–606. https://doi.org/10.1016/j.geotexmem.2022.02.006.
Lau, Z. C., A. Bouazza, and W. P. Gates. 2022b. "Water exchange across a subgrade-GCL interface as impacted by polymers and environmental conditions." *Geotext. Geomembr.* 50 (1): 40–54. https://doi.org/10.1016/j.geotexmem.2021.08.005.
Lee, J. M., and C. D. Shackelford. 2005. "Solution retention capacity as an alternative to the swell index test for sodium bentonite." *Geotech. Test. J.* 28 (1): 61–70. https://doi.org/10.1520/GTJ12520.
Li, X., J. H. Li, and L. M. Zhang. 2014. "Predicting bimodal soil–water characteristic curves and permeability functions using physically based parameters." *Comput. Geotech.* 57 (Apr): 85–96. https://doi.org/10.1016/j.compgeo.2014.01.004.
Liu, J., S. Song, X. Cao, Q. Meng, H. Pu, Y. Wang, and J. Liu. 2020. "Determination of full-scale pore size distribution of Gaomiaozi bentonite and its permeability prediction." *J. Rock Mech. Geotech. Eng.* 12 (2): 403–413. https://doi.org/10.1016/j.jrmge.2019.12.005.
Liu, Y., A. Bouazza, W. P. Gates, and R. K. Rowe. 2015. "Hydraulic performance of geosynthetic clay liners to sulfuric acid solutions." *Geotext. Geomembr.* 43 (1): 14–23. https://doi.org/10.1016/j.geotexmem.2014.11.004.
Lu, N. 2016. "Generalized soil water retention equation for adsorption and capillarity." *J. Geotech. Geoenviron. Eng.* 142 (10): 04016051. https://doi.org/10.1061/(ASCE)GT.1943-5606.0001524.
Lu, N., and M. Khorshidi. 2015. "Mechanisms for soil-water retention and hysteresis at high suction range." *J. Geotech. Geoenviron. Eng.* 141 (8): 04015032. https://doi.org/10.1061/(ASCE)GT.1943-5606.0001325.
Luo, S., and N. Lu. 2021. "Validating the generality of a closed-form equation for soil water isotherm." *J. Geotech. Geoenviron. Eng.* 147 (12): 04021138. https://doi.org/10.1061/(ASCE)GT.1943-5606.0002681.
Mazzieri, F., and G. Di Emidio. 2015. "Hydraulic conductivity of a dense prehydrated geosynthetic clay liner." *Geosynth. Int.* 22 (1): 138–148. https://doi.org/10.1680/gein.14.00037.
Nahlawi, H., A. Bouazza, and J. Kodikara. 2007. "Characterisation of geotextiles water retention using a modified capillary pressure cell." *Geotext. Geomembr.* 25 (3): 186–193. https://doi.org/10.1016/j.geotexmem.2006.12.001.
Navarro, V., L. Asensio, G. De la Morena, X. Pintado, and A. Yustres. 2015. "Differentiated intra-and inter-aggregate water content models of mx-80 bentonite." *Appl. Clay Sci.* 118 (Dec): 325–336. https://doi.org/10.1016/j.clay.2015.10.015.
Norrish, K. 1954. "The swelling of montmorillonite." *Discuss. Faraday Soc.* 18: 120–134. https://doi.org/10.1039/df9541800120.
Norrish, K., and J. T. Hutton. 1969. "An accurate X-ray spectrographic method for the analysis of a wide range of geological samples." *Geochim. Cosmochim. Acta* 33 (4): 431–453. https://doi.org/10.1016/0016-7037(69)90126-4.
Or, D., and M. Tuller. 2002. "Cavitation during desaturation of porous media under tension." *Water Resour. Res.* 38 (5): 1–14. https://doi.org/10.1029/2001WR000282.
Pasha, A. Y., A. Khoshghalb, and N. Khalili. 2017. "Hysteretic model for the evolution of water retention curve with void ratio." *J. Eng. Mech.* 143 (7): 04017030. https://doi.org/10.1061/(ASCE)EM.1943-7889.0001238.
Rayhani, M. T., R. K. Rowe, R. W. I. Brachman, W. A. Take, and G. Siemens. 2011. "Factors affecting GCL hydration under isothermal conditions." *Geotext. Geomembr.* 29 (6): 525–533. https://doi.org/10.1016/j.geotexmem.2011.06.001.
Revil, A., and N. Lu. 2013. "Unified water isotherms for clayey porous materials." *Water Resour. Res.* 49 (9): 5685–5699. https://doi.org/10.1002/wrcr.20426.
Romero, E., G. Della Vecchia, and C. Jommi. 2011. "An insight into the water retention properties of compacted clayey soils." *Géotechnique* 61 (4): 313–328. https://doi.org/10.1680/geot.2011.61.4.313.
Rouf, M. A., A. Bouazza, R. M. Singh, W. P. Gates, and R. K. Rowe. 2016a. "Water vapour adsorption and desorption in GCLs." *Geosynth. Int.* 23 (2): 86–99. https://doi.org/10.1680/jgein.15.00034.
Rouf, M. A., R. M. Singh, A. Bouazza, R. K. Rowe, and W. P. Gates. 2016b. "Gas permeability of partially hydrated geosynthetic clay liner under two stress conditions." *Environ. Geotech.* 3 (5): 325–333. https://doi.org/10.1680/envgeo.14.00009.
Rowe, R. K. 2014. "Performance of GCLs in liners for landfill and mining applications." *Environ. Geotech.* 1 (1): 3–21. https://doi.org/10.1680/envgeo.13.00031.
Rowe, R. K., and A. Y. AbdelRazek. 2021. "Performance of multi-component GCLs in high salinity impoundment applications." *Geotext. Geomembr.* 49 (2): 358–368. https://doi.org/10.1016/j.geotexmem.2020.10.007.
Rowe, R. K., M. T. Rayhani, W. A. Take, G. Siemens, and R. W. I. Brachman. 2011. "GCL hydration under simulated daily thermal cycles." *Geosynth. Int.* 18 (4): 196–205. https://doi.org/10.1680/gein.2011.18.4.196.

Sanchez, M., A. Gens, L. Guimaraes, and S. Olivella. 2006. "Response of an unsaturated expansive clay under high temperature changes." In *Unsaturated soils 2006*, 2488–2499. Reston, VA: ASCE.

Sánchez, M., A. Gens, M. V. Villar, and S. Olivella. 2016. "Fully coupled thermo-hydro-mechanical double-porosity formulation for unsaturated soils." *Int. J. Geomech.* 16 (6): D4016015. https://doi.org/10.1061/(ASCE)GM.1943-5622.0000728.

Sarabian, T., and M. T. Rayhani. 2013. "Hydration of geosynthetic clay liners from clay subsoil under simulated field conditions." *Waste Manage.* 33 (1): 67–73. https://doi.org/10.1016/j.wasman.2012.08.010.

Satyanaga, A., H. Rahardjo, E. C. Leong, and J. Y. Wang. 2013. "Water characteristic curve of soil with bimodal grain-size distribution." *Comput. Geotech.* 48 (Mar): 51–61. https://doi.org/10.1016/j.compgeo.2012.09.008.

Scalia, J., C. H. Benson, G. L. Bohnhoff, T. B. Edil, and C. D. Shackelford. 2014. "Long-term hydraulic conductivity of a bentonite-polymer composite permeated with aggressive inorganic solutions." *J. Geotech. Geoenviron. Eng.* 140 (3): 04013025. https://doi.org/10.1061/(ASCE)GT.1943-5606.0001040.

Seiphoori, A., A. Ferrari, and L. Laloui. 2014. "Water retention behaviour and microstructural evolution of MX-80 bentonite during wetting and drying cycles." *Géotechnique* 64 (9): 721–734. https://doi.org/10.1680/geot.14.P.017.

Seiphoori, A., L. Laloui, A. Ferrari, M. Hassan, and W. H. Khushefati. 2016. "Water retention and swelling behaviour of granular bentonites for application in geosynthetic clay liner (GCL) systems." *Soils Found.* 56 (3): 449–459. https://doi.org/10.1016/j.sandf.2016.04.011.

Shackelford, C. D., C. H. Benson, T. Katsumi, T. B. Edil, and L. Lin. 2000. "Evaluating the hydraulic conductivity of GCLs permeated with non-standard liquids." *Geotext. Geomembr.* 18 (2–4): 133–161. https://doi.org/10.1016/S0266-1144(99)00024-2.

Sumner, M. E., and W. P. Miller. 1996. "Cation exchange capacity and exchange coefficients." *Methods Soil Anal.: Part 3 Chem. Methods* 5: 1201–1229. https://doi.org/10.2136/sssabookser5.3.c40.

Tian, K., C. H. Benson, and W. J. Likos. 2016. "Hydraulic conductivity of geosynthetic clay liners to low-level radioactive waste leachate." *J. Geotech. Geoenviron. Eng.* 142 (8): 04016037. https://doi.org/10.1061/(ASCE)GT.1943-5606.0001495.

Tian, K., W. J. Likos, and C. H. Benson. 2019. "Polymer elution and hydraulic conductivity of bentonite–polymer composite geosynthetic clay liners." *J. Geotech. Geoenviron. Eng.* 145 (10): 04019071. https://doi.org/10.1061/(ASCE)GT.1943-5606.0002097.

Tincopa, M., and A. Bouazza. 2021. "Water retention curves of a geosynthetic clay liner under non-uniform temperature-stress paths." *Geotext. Geomembr.* 49 (5): 1270–1279. https://doi.org/10.1016/j.geotexmem.2021.04.005.

Tincopa, M., A. Bouazza, R. K. Rowe, and H. Rahardjo. 2020. "Back-analysis of the water retention curve of a GCL on the wetting path." *Geosynth. Int.* 27 (5): 523–537. https://doi.org/10.1680/jgein.20.00016.

Touze-Foltz, N., H. Bannour, C. Barral, and G. Stoltz. 2016. "A review of the performance of geosynthetics for environmental protection." *Geotext. Geomembr.* 44 (5): 656–672. https://doi.org/10.1016/j.geotexmem.2016.05.008.

Tuller, M., and D. Or. 2005. "Water films and scaling of soil characteristic curves at low water contents." *Water Resour. Res.* 41 (9): W09403. https://doi.org/10.1029/2005WR004142.

Van Genuchten, M. T. 1980. "A closed-form equation for predicting the hydraulic conductivity of unsaturated soils." *Soil Sci. Soc. Am. J.* 44 (5): 892–898. https://doi.org/10.2136/sssaj1980.03615995004400050002x.

Vasko, S., H. Y. Jo, C. H. Benson, T. B. Edil, and T. Katsumi. 2001. "Hydraulic conductivity of partially prehydrated geosynthetic clay liners permeated with aqueous calcium chloride solutions." In Vol. 2001 of *Proc., Geosynthetics Conf.*, 685–699. Roseville, MN: Industrial Fabrics Association International.

Villar, M. V., and A. Lloret. 2008. "Influence of dry density and water content on the swelling of a compacted bentonite." *Appl. Clay Sci.* 39 (1–2): 38–49. https://doi.org/10.1016/j.clay.2007.04.007.

Wijaya, M., and E. C. Leong. 2016. "Equation for unimodal and bimodal soil–water characteristic curves." *Soils Found.* 56 (2): 291–300. https://doi.org/10.1016/j.sandf.2016.02.011.

Wireko, C., B. Zainab, K. Tian, and T. Abichou. 2020. "Effect of specimen preparation on the swell index of bentonite-polymer GCLs." *Geotext. Geomembr.* 48 (6): 875–885. https://doi.org/10.1016/j.geotexmem.2020.06.006.

Yang, H., H. Rahardjo, E. C. Leong, and D. G. Fredlund. 2004. "Factors affecting drying and wetting soil-water characteristic curves of sandy soils." *Can. Geotech. J.* 41 (5): 908–920. https://doi.org/10.1139/t04-042.

Zhang, L., and Q. Chen. 2005. "Predicting bimodal soil–water characteristic curves." *J. Geotech. Geoenviron. Eng.* 131 (5): 666–670. https://doi.org/10.1061/(ASCE)1090-0241(2005)131:5(666).